Butterfly catastrophe for fronts in a three-component reaction-diffusion system

January 9, 2014

Martina Chirilus-Bruckner[1], Arjen Doelman[2], Peter van Heijster[3], Jens Rademacher[4]

Abstract

We study the dynamics of front solutions in a three-component reaction-diffusion system via a combination of geometric singular perturbation theory, Evans function analysis and center manifold reduction. The reduced system exhibits a surprisingly complicated bifurcation structure including a butterfly catastrophe. Our results shed light on numerically observed accelerations and oscillations and pave the way for the analysis of front interactions in a parameter regime where the essential spectrum of a single front approaches the imaginary axis asymptotically.

1 Introduction

The dynamics generated by systems of reaction-diffusion equations can be extremely complex. Nevertheless, even far from equilibrium, it is remarkably often the case that these dynamics can be viewed as being governed by the interactions of localized structures [Pe93, NU01]. Such structures are close to a trivial background state for the largest part of the spatial domain; the regions in which the solutions, or patterns, exhibit transitions between different background states, or to-and-from the same background state, are relatively small. Spots and stripes are typical examples of such localized structures in two space dimensions. In one space dimension, one can distinguish between fronts and pulses. Developing a mathematical understanding of the dynamics of reaction-diffusion equations far from equilibrium, i.e. in situations not close to bifurcations of a trivial state that are governed by small-amplitude dynamics, is most often centered around these localized structures. Moreover, this approach has the nature of a three-step process: first one focuses on establishing the existence of simple – stationary, or traveling with a constant speed – localized structures, followed by a spectral stability analysis. Based on that, one can begin the study of interactions between these objects.

[1]Division of Applied Mathematics, Brown University, 182 George Street, Providence, RI 02912, USA;
School of Mathematics and Statistics, University of Sydney, Carslaw Building F07, Sydney NSW 2008, Australia

[2]Mathematisch Instituut, Leiden University, P.O. Box 9512, 2300 RA Leiden, the Netherlands

[3]Mathematical Sciences School, Queensland University of Technology GPO Box 2434, Brisbane, Qld 4001, Australia

[4]Universiät Bremen, Fachbereich Mathematik, Postfach 22 04 40, 20359 Bremen, Germany

In recent years, significant progress has been made within all three steps of this approach, especially in the context of singularly perturbed systems in one spatial dimension, see for instance [CW09, DKP07, vHDKP10, Ra13, SRW05] and the references therein, or for structures with (at leading order) some kind of internal symmetry – circular spots, planar fronts and/or stripes – in two space dimensions, see [vHS11, KWW06, KWY13] and the references therein. In fact, there is a quite well-developed general theory for the *weak interactions* of pulses and fronts in one spatial dimension [Ei02, EMN02, Pro02, Sa02]. Here *weak* refers to the condition that two interacting structures should be *sufficiently far* removed from each other; more explicitly, in the weak case the dynamics are driven by the interactions between the exponentially small 'tails' of the fronts/pulses. As a consequence, these weak dynamics are exponentially slow and, hence, the dynamical richness is rather limited. For instance fronts/pulses cannot change shape within the weak limit, nor can their stability type be influenced by weak interactions. This only happens when the fronts/pulses are *too close to each other*, i.e., in the *strong* interaction case. There is, however, no mathematical theory for strong interactions in reaction-diffusion systems.

To extend the class of systems and/or phenomena that can be studied analytically, the concept of *semi-strong interactions* was introduced in [DK03] in the context of singularly perturbed systems. In a singularly perturbed system, one distinguishes between (relatively) *large* and *small* diffusion coefficients; the fast components only vary on (relatively) short spatial scales and are associated to the small diffusion coefficients, the slow components, associated to large diffusivities, change on longer spatial scales. By definition, fronts/pulses are in semi-strong interaction if the fast components of the localized structures are in a weak, exponentially small tail-tail interaction, while the slow components are coupled in a strong way (and thus not only through tail-tail interactions). Semi-strong interaction dynamics are much richer than weak interaction dynamics, fronts/pulses change their shape and nature, they may bifurcate and even blow-up in finite time. Moreover, the renormalization group approach that was originally developed in the context of weak interactions [Pro02] has been extended to the semi-strong setting in a sequence of papers [DKP07, vHDKP10, BDKP13]: in these papers it is shown that if the essential spectrum associated to a solitary front/pulse is *not too close* to the origin of the complex plane, a bootstrap-like method can be devised by which both the validity and the nonlinear stability, or (local) attractivity, of the front/pulse-dynamics can be established rigorously.

Naturally, a central issue in obtaining a deeper understanding of (semi-strong) pulse dynamics is the question about the impact of having essential spectrum too close to the imaginary axis. Simulations in [DvHK09, vHDK08, vHDKP10] strongly indicate that the richness of the (semi-strong) pulse dynamics greatly increases as the essential spectrum moves closer to the imaginary axis. Moreover, the formal approach of [DK03], originally developed in [DEK01], by which the (leading order) front/pulse interaction equations can be derived in a geometrical way, also breaks down under these same circumstances – while the essential spectrum itself does not appear at all in this method (see also [DEK01, DK03, DKP07, vHDKP10]). Moreover, the character of the equations derived by this method cannot describe the phenomena exhibited by the localized structures as the essential spectrum approaches the origin. In particular, the N-front interaction equations obtained and validated in [vHDKP10] have a gradient structure, and thus cannot govern Hopf bifurcations. However, Hopf bifurcations do appear in the (PDE) dynamics beyond the range of validity of the renormalization group approach [vHDKP10]. Thus we are led to conclude that the condition on *not being too close* that underpins the renormalization group approach of [DKP07, vHDKP10, BDKP13] may not be

a technical condition: the essential spectrum – or, better – its closeness to the origin, may have a significant impact on the dynamics of fronts/pulses.

This issue is the underlying motivation for the research presented in this paper. To facilitate and focus our investigation, we consider the same FitzHugh-Nagumo type system of reaction-diffusion equations as in [DvHK09, vHDK08, vHDKP10],

$$\left\{\begin{array}{rcrl} U_t &=& \varepsilon^2 U_{xx} &+ U - U^3 - \varepsilon(\alpha V + \beta W + \gamma)\,, \\ \tau V_t &=& V_{xx} &+ U - V\,, \\ \theta W_t &=& D^2 W_{xx} &+ U - W\,, \end{array}\right.$$

for the three real-valued components U, V, W, each depending on $(x,t) \in \mathbb{R} \times \mathbb{R}_+$. For the system parameters $\varepsilon, \alpha, \beta, \gamma, \tau, \theta, D \in \mathbb{R}$, we assume $\tau, \theta > 0, D > 1$ and that $0 < \varepsilon \ll 1$, that is, ε plays the distinguished role of a small perturbation parameter, and determines that the U-component is *fast*, while the V- and W-components are *slow*. Apart from its importance in the theory of pattern formation (cf. [NTU03, NTYU07, VE07, CC12]), this system has previously been suggested as phenomenological model for gas-discharge (cf. [SOBP97, NTU03, DvHK09] and the references therein).

In this system, localized structures have a front, or multi-front, character [DvHK09]: the system is bi-stable with 2 stable trivial background states at leading order in ε given by $(U,V,W) = \pm(1,1,1)$. Clearly, the parameters τ and θ directly control the position of the essential spectrum associated to front solutions connecting these states. In [vHDKP10], the dynamics of N interacting fronts is studied analytically under the condition that τ and θ are $\mathcal{O}(1)$ with respect to ε. In this paper, we focus on the parameter regime

$$\tau = \frac{\hat{\tau}}{\varepsilon^2}, \quad \theta = \frac{\hat{\theta}}{\varepsilon^2}, \qquad \hat{\tau}, \hat{\theta} > 0,$$

that is, where τ and θ are large, so the essential spectrum associated to front-type solutions is close, in fact $\mathcal{O}(\varepsilon^2)$-close, to the imaginary axis. This is the setting in which the renormalization group approach breaks down and in which the three-component system exhibits particularly rich dynamics (in fact the methods break down as soon as τ, θ become $\gg 1$ – see [vHDK08] for a brief discussion of the transition case $1 \ll \tau, \theta \ll 1/\varepsilon^2$).

An analytical explanation of both the observed complex dynamics and the encountered analytical challenges in these parameter regimes begins by going back to the start of the above sketched three-step process, that is, by developing a full understanding of the building blocks of these more complicated structures: single fronts. This is the subject of the present work. We will find that in this setting even a single front can exhibit unexpectedly rich dynamics such as accelerations and oscillations – much richer than the solitary front dynamics for $\tau, \theta = \mathcal{O}(1)$. This already provides a first step in explaining the rich semi-strong front interaction dynamics for large τ and/or θ [NTU03, NTYU07, DvHK09].

In the subsequent analysis, we set $\tau = \frac{\hat{\tau}}{\varepsilon^2}, \theta = \frac{\hat{\theta}}{\varepsilon^2}$, with $\hat{\tau}, \hat{\theta} > 0$, and examine front solutions of the

rescaled system

$$\begin{cases} U_t &= \varepsilon^2 U_{xx} &+ U - U^3 - \varepsilon(\alpha V + \beta W + \gamma)\,, \\ \hat{\tau} V_t &= \varepsilon^2 V_{xx} &+ \varepsilon^2 (U - V)\,, \\ \hat{\theta} W_t &= \varepsilon^2 D^2 W_{xx} &+ \varepsilon^2 (U - W)\,. \end{cases} \tag{1.1}$$

Since the specific scaling of τ and θ causes all diffusion coefficients to be of equal asymptotic scaling, it is more natural to work with the rescaled spatial scale $\xi = \frac{x}{\varepsilon}$ for which (1.1) becomes

$$\begin{cases} U_t &= U_{\xi\xi} &+ U - U^3 - \varepsilon(\alpha V + \beta W + \gamma)\,, \\ \hat{\tau} V_t &= V_{\xi\xi} &+ \varepsilon^2 (U - V)\,, \\ \hat{\theta} W_t &= D^2 W_{\xi\xi} &+ \varepsilon^2 (U - W)\,. \end{cases} \tag{1.2}$$

This system is equivalent to (1.1) for $\varepsilon \neq 0$. Note that, despite the equal scaling of all three diffusion coefficients, the different scaling in the reaction terms still gives rise to a traveling wave ODE with slow/fast structure (see (2.1) and (2.3)).

The existence of fronts comes as no surprise since the (dominating) U component solves an Allen-Cahn/Nagumo type equation for which the existence of front solutions is well-known. The problem at hand is indeed similar to the perturbed bi-stable equation

$$\partial_t U = \varepsilon^2 \partial_x^2 U + U - U^3 - \varepsilon\gamma, \tag{1.3}$$

which is known to feature fronts connecting the homogeneous background states $-1 + \mathcal{O}(\varepsilon)$ and $+1 + \mathcal{O}(\varepsilon)$, whose interface becomes sharper as $\varepsilon \to 0$ and which travel with speed $\mathcal{O}(\varepsilon^2\gamma)$ (cf. [CP89] and [FH89]).

Outline and main results

The present work is organized in three parts. In Section 2, we treat the existence problem for uniformly traveling front solutions (see left panel of Figure 1). An existence result (see Proposition 2.2) is presented featuring existence condition (2.10) which reads

$$\frac{1}{3}\sqrt{2}\, c = \alpha\, v_* + \beta\, w_* + \gamma\,, \quad v_* = v_*(c;\hat{\tau})\,, w_* = w_*(c;\hat{\theta}, D)\,, \tag{1.4}$$

that arises from Melnikov analysis and relates the front speed $\varepsilon^2 c$ (in the slow variable x) with the system parameters. The construction involves geometric singular perturbation theory w.r.t. $0 < \varepsilon \ll 1$ (cf. [Jo95]) closely following the construction in [DvHK09], where it was demonstrated that a uniformly traveling pulse constructed as a two-front with width ξ_* exists for parameter constellations which reduce to our condition (1.4) for $\xi_* \to \infty$ (see [DvHK09] for more details). To keep the exposition at reasonable length, we therefore choose to omit the proof and rather simply delineate the construction of fronts followed by a thorough analysis of the bifurcation structure that the existence condition reveals. We find the imprint of a partially unfolded butterfly catastrophe (see Lemma 2.5 and Figure 1 or Figure 6). Thus, the existence problem has a remarkably rich

structure with the possible coexistence of up to five fronts with different velocities (see Lemma 3.9).

In Section 3 we discuss the stability of uniformly traveling fronts which turns out to be decided by the so-called *small eigenvalues* $\lambda = \varepsilon^2\hat{\lambda}$. Based on an explicit computation of the (leading order) Evans function, we give in Theorem 3.4 relation (3.6) for the small eigenvalues reading

$$-\frac{\sqrt{2}}{6}\hat{\lambda} + \alpha F_{c\hat{\tau},\hat{\tau}}(\hat{\lambda}) + \frac{\beta}{D}F_{c\hat{\theta}/D,\hat{\theta}}(\hat{\lambda}) = 0\,.$$

Note that, even though our proof strategy follows [vHDK08], which discusses stability of multifront solutions, the derivation of the stability result for the single front in the present setting needed substantial modifications. Moreover, [vHDK08] does not discuss the entire parameter regime. For transparency of presentation, the details of the (spectral) stability analysis are postponed to Appendix B.

Despite the complexity of the derived eigenvalue relation (3.6), it is possible to prove (see Appendix C) that there are at most three small eigenvalues, of which zero is always one due to the translation invariance of our system (see Lemma 3.6). This can be directly translated into the expected dynamics of bifurcating fronts. Put differently, a center manifold reduction at onset of instability will lead to a system whose dimension is at most two (after factoring out the translation invariance).

The findings of our stability analysis pave the way for Section 4 where we use center manifold reduction to describe dynamically evolving fronts bifurcating from stationary ones (see Theorem 4.1). To simplify the exposition, we choose to execute the reduction and unfolding for a special parameter regime which results in a scalar reduced equation rather than a two-dimensional system as in the general case.

We conclude the paper with a discussion of consequences and future directions. Directly in line with the center manifold analysis of Section 4, the most interesting investigation is the exploration of the parameter regimes that allow both a triple zero eigenvalue and the butterfly catastrophe (see Lemma 3.9), which together foreshadow a possible Bogdanov-Takens bifurcation with butterfly imprint. We also return to the above described phenomena that motivated our research and discuss the potential impact of our findings on the three-step process underlying our approach to understanding the (semi-strong) interactions of localized structures.

Remark 1.1. *Note that the findings of our work clearly highlight the importance of having a third component in the linearly coupled system (1.1). Without its presence (that is, for $\beta = 0$) the bifurcation structure collapses to a common cusp bifurcation (as, for instance, described in [KNO90] or [EIK08]) and the reduced equation on the center manifold is always one-dimensional. In particular, the Hopf bifurcation (see Figure 11) that gives rise to oscillating fronts is not possible for the corresponding two-component system*

$$\begin{cases} U_t &= \varepsilon^2 U_{xx} &+ U - U^3 - \varepsilon(\alpha V + \gamma)\,, \\ \tau V_t &= V_{xx} &+ U - V\,. \end{cases}$$

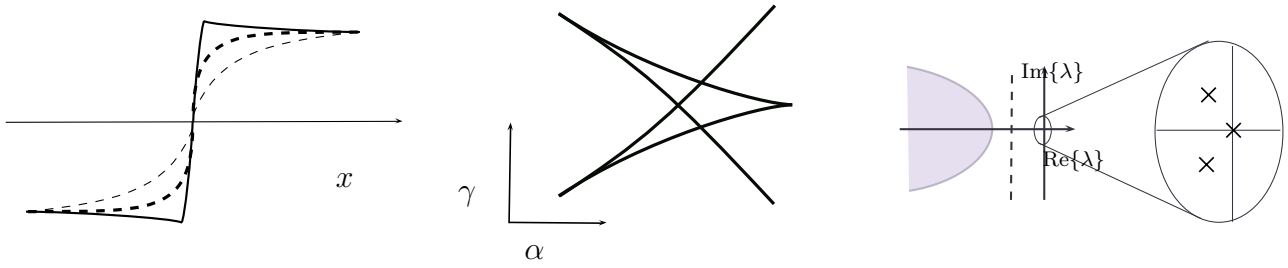

FIGURE 1: *Left panel*: Spatial profile of a stationary front solution (U solid, V, W dashed). *Middle panel*: Butterfly catastrophe for traveling fronts bifurcating from stationary ones. *Right panel*: Spectrum of the linearization around traveling fronts.

Acknowledgements
The work of M.C.-B. is supported by the Deutsche Forschungsgemeinschaft (DFG) under the grant CH 957/1-1. J.R. is grateful for the support of the Dutch NWO cluster NDNS+ and his previous employer, Centrum Wiskunde & Informatica (CWI), Amsterdam. P.v.H. is grateful for the support of his previous employer, Boston University, Boston. The authors would like to thank Björn Sandstede for inspiring discussions.

2 Existence of stationary and uniformly traveling fronts

To study the existence of uniformly traveling front solutions we choose a comoving frame $y = x - \varepsilon^2 ct, c \in \mathbb{R}$, and insert the traveling wave ansatz

$$(U, V, W)(x, t) = (u, v, w)(x - \varepsilon^2 ct),$$

into (1.1) to arrive at a traveling wave ODE that we write as first-order system

$$\begin{cases} \varepsilon u' &= p\,, \\ \varepsilon p' &= -u + u^3 + \varepsilon(\alpha v + \beta w + \gamma - cp)\,, \\ v' &= q\,, \\ q' &= v - u - c\hat{\tau} q\,, \\ w' &= \frac{r}{D}\,, \\ r' &= \frac{1}{D}(w - u) - c\frac{\hat{\theta}}{D^2} r\,, \end{cases} \tag{2.1}$$

where $\cdot' = \frac{d}{dy}$. The relevant fixed points of this system are given by

$$P_\varepsilon^\pm = (u_\varepsilon^\pm, 0, u_\varepsilon^\pm, 0, u_\varepsilon^\pm, 0), \qquad u_\varepsilon^\pm = \pm 1 \mp \frac{1}{2}\varepsilon(\alpha + \beta \pm \gamma) + \mathcal{O}(\varepsilon^2)\,. \tag{2.2}$$

Heteroclinic connections between them correspond to uniformly traveling fronts of (1.1). The ODE system (2.1) is singularly perturbed and, hence, can be viewed as a *slow* system whose *fast* counter part associated with the *fast scale* $\eta = \frac{x - \varepsilon^2 ct}{\varepsilon} = \frac{y}{\varepsilon}$ is of the form (differentiation now being understood

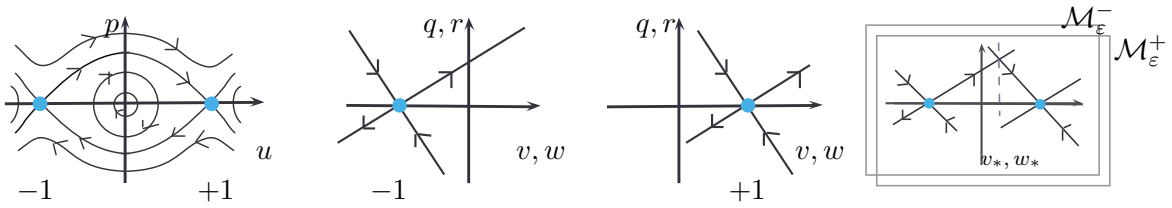

FIGURE 2: *Left panel*: Phase portrait for $\ddot{u} = -u + u^3$. *Middle panels*: Phase portraits for the slow components in (2.6) with $u = +1$ and $u = -1$. *Right panel*: $v_* = l_v^{\mathrm{u}}(-1) \cap l_v^{\mathrm{s}}(+1), w_* = l_w^{\mathrm{u}}(-1) \cap l_w^{\mathrm{s}}(+1)$.

w.r.t. η)

$$\begin{cases} \dot{u} &= p\,, \\ \dot{p} &= -u + u^3 + \varepsilon(\alpha v + \beta w + \gamma - cp)\,, \\ \dot{v} &= \varepsilon q\,, \\ \dot{q} &= \varepsilon(v - u) - \varepsilon c\hat{\tau} q\,, \\ \dot{w} &= \frac{\varepsilon}{D} r\,, \\ \dot{r} &= \frac{\varepsilon}{D}(w - u) - \frac{\varepsilon}{D^2} c\hat{\theta} r\,. \end{cases} \tag{2.3}$$

Systems (2.1) and (2.3) are equivalent for $\varepsilon \neq 0$ and geometric singular perturbation theory can be employed to construct a heteroclinic orbit from the different limiting equations for (2.1) and (2.3) when $\varepsilon \to 0$. Setting $\varepsilon = 0$ in (2.3) gives the fast reduced system

$$\begin{cases} \dot{u} &= p\,, \\ \dot{p} &= -u + u^3, \\ \dot{v} &= \dot{q} = \dot{w} = \dot{r} = 0\,, \end{cases} \tag{2.4}$$

whose equation for the u-component is known to have a pair of heteroclinic solutions connecting -1 and $+1$ (see Figure 2, left panel) given by

$$(u_{0,\pm}(\eta), p_{0,\pm}(\eta)) = \pm\left(\tanh\left(\frac{\eta}{\sqrt{2}}\right), \frac{1}{\sqrt{2}}\operatorname{sech}^2\left(\frac{\eta}{\sqrt{2}}\right)\right). \tag{2.5}$$

This provides the core of the heteroclinic orbit for the full system and, therefore, for the front solution of our PDE system (1.1). Setting $\varepsilon = 0$ in (2.1) gives the slow reduced system

$$\begin{cases} 0 &= -u + u^3\,, \\ v' &= q\,, \\ q' &= v - u - \hat{\tau} c q\,, \\ w' &= \frac{r}{D}\,, \\ r' &= \frac{1}{D}(w - u) - \frac{\hat{\theta}}{D^2} c r\,. \end{cases} \tag{2.6}$$

Its solutions are obtained by solving the (v, q, w, r)-equations on the manifolds

$$\mathcal{M}_0^{\pm} = \{(u, p, v, q, w, r) \mid u = \pm 1, p = 0\}\,.$$

As illustrated in Figure 2 (middle panels) these equations possess saddle equilibria at $(v,q)=(\pm1,0)$ or $(w,r)=(\pm1,0)$ respectively with stable and unstable manifolds (corresponding in this case to the eigenspaces)

$$l_v^{\mathrm{u/s}}(u_0)=\left\{(v,q)\mid q=\lambda_v^{\pm}(v-u_0)\right\},\quad l_w^{\mathrm{u/s}}(u_0)=\left\{(w,r)\mid r=D\lambda_w^{\pm}(w-u_0)\right\},\ u_0=\pm1$$

with $u_0=+1$ or $u_0=-1$ and

$$\lambda_{v,\pm}=\frac{1}{2}\left(-c\hat{\tau}\pm\sqrt{c^2\hat{\tau}^2+4}\right),\quad \lambda_{w,\pm}=\frac{1}{2D}\left(-c\widetilde{\theta}\pm\sqrt{c^2\widetilde{\theta}^2+4}\right),\quad \frac{\hat{\theta}}{D}=:\widetilde{\theta}.$$

Remark 2.1. *Note that, for the existence analysis, the parameters $\hat{\theta}$ and D only appear as $\frac{\hat{\theta}}{D}=\widetilde{\theta}$, while for the stability analysis in the next section $\hat{\theta}$ and D have distinguished roles.*

In the following we will denote the corresponding manifolds in the full phase space by

$$\Lambda_{\pm1}^{\mathrm{u/s}}=\left\{(u,p,v,q,w,r)\mid(v,q,w,r)\in l_v^{\mathrm{u/s}}(\pm1)\times l_w^{\mathrm{u/s}}(\pm1)\right\}.$$

Associated with the slow and fast systems (2.1) and (2.3) are the slow and fast intervals that we define w.r.t. the fast variable η, that is,

$$I_{s,-}=\left(-\infty,-\frac{1}{\sqrt{\varepsilon}}\right),\ I_f=\left[-\frac{1}{\sqrt{\varepsilon}},+\frac{1}{\sqrt{\varepsilon}}\right],\ I_{s,+}=\left(+\frac{1}{\sqrt{\varepsilon}},+\infty\right).\tag{2.7}$$

A crucial observation is that the (v,q,w,r)-components are constant to leading order during the jump from $\mathcal{M}_0^-$ to $\mathcal{M}_0^+$ (while the (u,p)-components are described to leading order by (2.5)). This is due to the fact that, in the fast interval I_f, we have

$$v\left(+\frac{1}{\sqrt{\varepsilon}}\right)-v\left(-\frac{1}{\sqrt{\varepsilon}}\right)=\int_{I_f}\dot{v}(\eta)\,d\eta=\mathcal{O}(\sqrt{\varepsilon})$$

and similarly for the (q,w,r)-components (cf. [DvHK09] for details). This motivates the right panel in Figure 2 according to which these constant values are obtained from the intersection of $l_v^{\mathrm{u}}(-1)$ and $l_v^{\mathrm{s}}(+1)$ (resp. $l_w^{\mathrm{u}}(-1)$ and $l_w^{\mathrm{s}}(+1)$), that is,

$$(v_*,q_*)=l_v^{\mathrm{u}}(-1)\cap l_v^{\mathrm{s}}(+1),\quad (w_*,r_*)=l_w^{\mathrm{u}}(-1)\cap l_w^{\mathrm{s}}(+1),$$

which can be determined explicitly to be given by

$$v_*=\frac{c\hat{\tau}}{\sqrt{c^2\hat{\tau}^2+4}},\quad w_*=\frac{c\widetilde{\theta}}{\sqrt{c^2\widetilde{\theta}^2+4}},\tag{2.8}$$

where again, $\widetilde{\theta}=\frac{\hat{\theta}}{D}$. It is worth remarking already at this point that (2.8) shows that the sign of the jump values of v_*,w_* coincides with the sign of the velocity c. In particular, $v_*,w_*=0$ for stationary fronts.

We can now construct a singular orbit (corresponding to a heteroclinic from -1 to $+1$)

$$z_{\mathrm{het}}^0\ =\ z_{\mathrm{het;s,-}}^0\ \cup\ z_{\mathrm{het;f}}^0\ \cup\ z_{\mathrm{het;s,+}}^0\tag{2.9}$$

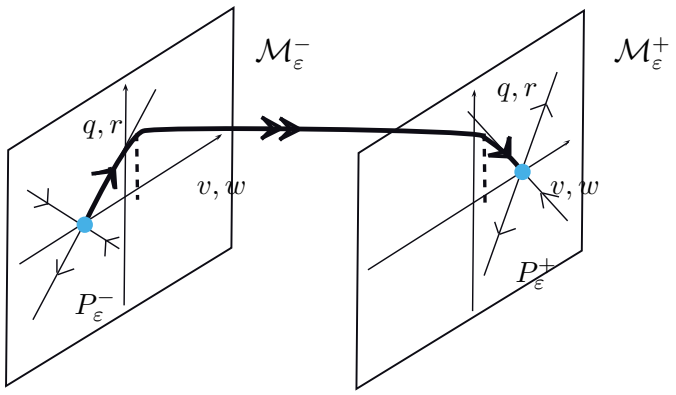

FIGURE 3: Schematic picture of the heteroclinic orbit $Z^\varepsilon_{\rm het}$ of the full system (2.1), stressing that, for $\varepsilon \to 0$, the heteroclinic orbit approaches $\mathcal{M}_0^\pm$, each a manifold given by the product of two planes corresponding to the (v, q) and (w, r) coordinates, respectively.

whose three parts are given by

$$\begin{aligned} z^0_{\rm het;s,-} &= \{(u,p,v,q,w,r) \in \mathcal{M}_0^- \cap \Lambda^{\rm u}_{-1} \mid -1 \le v \le v_*, -1 \le w \le w_*\}, \\ z^0_{\rm het;f} &= \{(u,p,v_*,q_*,w_*,r_*) \mid u = u_{0,+}(\eta), p = p_{0,+}(\eta), \eta \in \mathbb{R}\}, \\ z^0_{\rm het;s,+} &= \{(u,p,v,q,w,r) \in \mathcal{M}_0^+ \cap \Lambda^{\rm s}_{+1} \mid v_* \le v \le +1, w_* \le w \le +1\}. \end{aligned}$$

A heteroclinic orbit $z^\varepsilon_{\rm het}$ of the full system (2.1) connecting P_ε^- to P_ε^+ lies in the intersection of the unstable manifold $\mathcal{W}^u(P_\varepsilon^-)$ of P_ε^- and the stable manifold $\mathcal{W}^s(P_\varepsilon^+)$ of P_ε^+. Since $\dim(\mathcal{W}^s(P_\varepsilon^\pm)) = 3$ and the phase space is 6-dimensional, we will use the parameter c to create a one-dimensional intersection. Exploiting the Hamiltonian nature of the (u-equation of the fast reduced) system $\ddot{u} = -u + u^3$, we can construct a Melnikov function which will yield an implicit relation for c that guarantees the persistence of the heteroclinic orbits (2.5) of the reduced fast system (see Figure 2, left panel) into the regime $\varepsilon > 0$. Formal analysis by means of regular expansions and matching for the slow and fast systems (2.1) and (2.3) yield the existence condition $\alpha v_* + \beta w_* + \gamma - \frac{\sqrt{2}}{3} c = 0$, where v_*, w_* are the values of the (v, w)-components in the fast field (see (2.8)). Combining Fenichel theory and Melnikov analysis this existence condition can be derived rigorously. In fact, one can prove an existence result for uniformly traveling fronts by closely following [vHDK08]. Hence, we simply state the result and omit the proof here.

Proposition 2.2. (Existence of stationary and uniformly traveling fronts)
For any bounded set of $\alpha, \beta, \hat{\tau}, \hat{\theta}, D, \gamma, c$ there is $\varepsilon_0 > 0$ and an open neighborhood $\mathcal{U} \subset \mathbb{R}^6$ of the singular orbit $z^0_{\rm het}$ from (2.9) such that for all $\varepsilon \in (0, \varepsilon_0)$ solutions to

$$\Gamma_0(c) := \alpha \left(\frac{c\hat{\tau}}{\sqrt{c^2\hat{\tau}^2 + 4}} \right) + \beta \left(\frac{c\widetilde{\theta}}{\sqrt{c^2\widetilde{\theta}^2 + 4}} \right) + \gamma - \frac{\sqrt{2}}{3} c = 0, \quad \widetilde{\theta} = \frac{\hat{\theta}}{D}, \tag{2.10}$$

are in one-to-one correspondence with heteroclinic orbits

$$z^\varepsilon_{\rm het} = (u^\varepsilon_{\rm het}, p^\varepsilon_{\rm het}, v^\varepsilon_{\rm het}, q^\varepsilon_{\rm het}, w^\varepsilon_{\rm het}, r^\varepsilon_{\rm het})$$

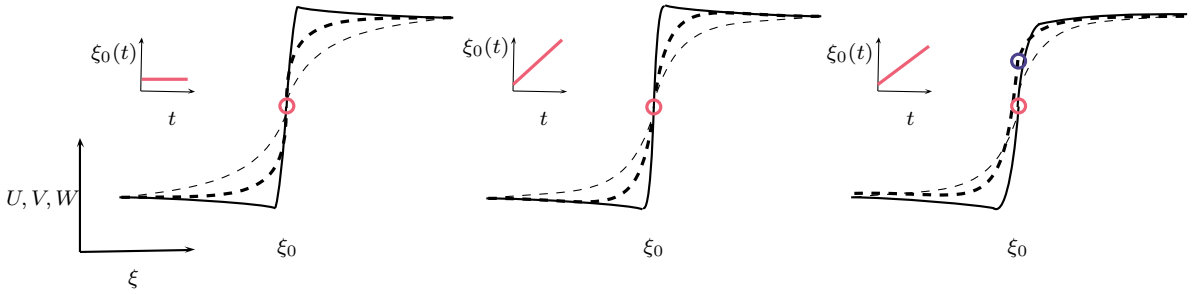

FIGURE 4: *Large plots*: Spatial profile of a front solution (U solid, V, W dashed). *Small plots*: Trajectory of the front represented by the space-time plot of the zero-crossing ξ_0 of the U-component. *Parameter settings*: $\varepsilon = 0.03, \beta = 3, \theta = 1, D = 3$ with varying γ, τ, α. *Left panel*: $\gamma = 0, \tau = 1, \alpha = 0.6428$. *Middle panel*: $\gamma = 1, \tau = 1, \alpha = 0.6428$. *Right panel*: $\gamma = 0, \tau = \frac{1}{\varepsilon^2}, \alpha = 1.2428$. Numerical computations where carried out by a moving grid code (cf. [Zeg07])

.

of (2.1) *that lie in* $\mathcal{U}$ *and connect* P_ε^- *to* P_ε^+ *from* (2.2). *Moreover, for each* $x \in \mathbb{R}$ *we have that*

$$\operatorname{dist}\left(z^\varepsilon_{\mathrm{het}}(x), z^0_{\mathrm{het}}\right) \longrightarrow 0\,, \quad \varepsilon \longrightarrow 0\,,$$

and the dependence of $z^\varepsilon_{\mathrm{het}}$ *on* ε *is smooth for each fixed* $x \in \mathbb{R}$. *These heteroclinics give rise to uniformly traveling fronts*

$$Z_{\mathrm{tf}}(x,t) = (U_{\mathrm{tf}}, V_{\mathrm{tf}}, W_{\mathrm{tf}})(x,t) = (u_{\mathrm{het}}(x - \varepsilon^2 ct), v_{\mathrm{het}}(x - \varepsilon^2 ct), w_{\mathrm{het}}(x - \varepsilon^2 ct)) \tag{2.11}$$

for the three-component system (1.1), *which are unique in* $\mathcal{U}$. *In particular, stationary fronts* Z_{sf}, *that is,* Z_{tf} *with* $c = 0$, *exist if and only if* $\gamma = 0$ *and* Z_{sf} *is an odd function of* x.

Corollary 2.3. *The leading order expression of* $(u^\varepsilon_{\mathrm{het}}, v^\varepsilon_{\mathrm{het}}, w^\varepsilon_{\mathrm{het}})$ *is given by*

$$\begin{bmatrix} -1 \\ (v_*+1)e^{\lambda_v^+ y} - 1 \\ (w_*+1)e^{\lambda_w^+ y} - 1 \end{bmatrix} \chi_{s-}(y) + \begin{bmatrix} \tanh\left[\frac{y}{\sqrt{2}\varepsilon}\right] \\ v_* \\ w_* \end{bmatrix} \chi_f(y) + \begin{bmatrix} +1 \\ (v_*-1)e^{\lambda_v^- y} + 1 \\ (w_*-1)e^{\lambda_w^- y} + 1 \end{bmatrix} \chi_{s+}(y)$$

where $\chi_{s-} = \chi_{\left(-\infty,-\sqrt{\varepsilon}\right)}, \chi_f = \chi_{\left[-\sqrt{\varepsilon},+\sqrt{\varepsilon}\right]}, \chi_{s+} = \chi_{\left(+\sqrt{\varepsilon},+\infty\right)}$ *are the characteristic functions for the three different intervals in the slow variable.*

For the stability analysis in the next section we will need some information on the higher order correction terms of $z^\varepsilon_{\mathrm{het}}$. They are described in Appendix A.

2.1 Parameters and front properties

Recall that for the Allen-Cahn equation (1.3) the velocity of fronts is proportional to γ. In particular, $\gamma = 0$ implies $c = 0$. This structure carries over to our system (1.1) as long as $\tau, \theta = \mathcal{O}(1)$ (see left panel of Figure 4 for a stationary front with $\gamma = 0$ and middle panel of Figure 4 for a

front traveling with velocity $c = \mathcal{O}(\gamma)$). However, for large τ, θ, fixing $\gamma = 0$ does not necessary imply $c = 0$, since the existence condition (2.10) can have more than just the trivial solution $c = 0$. Hence, traveling fronts can coexist with the stationary one. Such a traveling front in this regime is depicted in the right panel of Figure 4.

We will explain the underlying pitchfork bifurcations later on (in Section 2.2), but would like to already stress at this point that one can see from the front profiles in Figure 4 that the pitchfork bifurcation caused by γ does not alter the front profile qualitatively (compare left and middle panel of Figure 4), while for large τ and/or θ, if $c = 0$ then $v_* = w_* = 0$, and if $c \lesseqgtr 0$, then $\mp 1 \lesseqgtr v_* \lesseqgtr 0$ and $\mp 1 \lesseqgtr w_* \lesseqgtr 0$. In other words, the sign of the velocity coincides with the sign of the jump values v_*, w_* (see right panel of Figure 4). This agrees with the interpretation that γ is a forcing term whereas the rest of the parameters are expected to create traveling fronts through instabilities.

Examining our existence condition (2.10) reveals the possible coexistence of up to five fronts with different velocities (see Figure 5 for a respective parameter regime).

Lemma 2.4. (Number of coexisting fronts) *The existence condition* (2.10) *has* $n = \{1, 3, 5\}$ *solutions counted with multiplicity. In more detail,*

(i) if $\alpha\beta \geq 0$ *and* $\alpha\hat{\tau} + \frac{\beta}{D}\hat{\theta} < \frac{2\sqrt{2}}{3}$*, then* $n = 1$*,*

(ii) $n = 5$ *requires* $\alpha\beta < 0$*.*

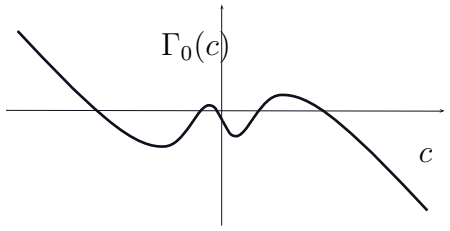

FIGURE 5: Existence function Γ_0 in (2.10) with parameters $\alpha = -0.61, \beta = 1.4023, \gamma = -0.05, \hat{\tau} = 10, \hat{\theta} = 5$ and $D = 2$ where five traveling fronts coexist.

Proof. We first note that $\Gamma_0(c) - \gamma$ is a smooth odd function with respect to c and $\lim_{c\to\pm\infty} \Gamma_0(c) = \mp\infty$. Hence, the number of roots of $\Gamma_0(c) = 0$ (counted with multiplicity) is odd. Second, we have

$$\frac{\mathrm{d}^2}{\mathrm{d}c^2}\Gamma_0(c) = -12c\left(\frac{\alpha\hat{\tau}^3}{(c^2\hat{\tau}^2+4)^{5/2}} + \frac{\beta(\hat{\theta}/D)^3}{(c^2(\hat{\theta}/D)^2+4)^{5/2}}\right)$$

so that inflection points of Γ_0 lie at $c = 0$ and at roots of the second factor. The latter requires $\alpha\beta \leq 0$ and

$$c^2 = -4\frac{(\alpha\hat{\tau}^3)^{2/5} + (\beta(\hat{\theta}/D)^3)^{2/5}}{(\hat{\theta}/D)^2(\alpha\hat{\tau}^3)^{2/5} + \tau^2(\beta(\hat{\theta}/D)^3)^{2/5}}. \tag{2.12}$$

In conclusion, if $\alpha\beta < 0$, then Γ_0 has three inflection points, hence, at most five roots. If $\alpha\beta > 0$, then Γ_0 has a unique inflection point and therefore at most three roots. Since $\lim_{c\to\pm\infty}\Gamma_0(c) = \mp\infty$, the unique inflection point at $c = 0$ for $\alpha\beta \geq 0$ further implies a unique zero of Γ_0 in case $\frac{\mathrm{d}}{\mathrm{d}c}\Gamma_0(0) < 0$. Indeed, the condition of item (i) implies

$$\frac{\mathrm{d}}{\mathrm{d}c}\Gamma_0(0) = \frac{1}{2}\left(\alpha\hat{\tau} + \frac{\beta}{D}\hat{\theta} - \frac{\sqrt{2}}{3}\right) < 0.$$

□

2.2 A butterfly catastrophe

We now examine the bifurcation structure in detail. It turns out that one can find the normal form of a partially unfolded butterfly catastrophe (see [PS96]) by expanding the existence condition (2.10) around $c = 0$, that is,

$$0 = \Gamma_0(c) = \gamma + \frac{1}{2}\kappa_1 c + \frac{1}{16}\kappa_3 c^3 + \frac{3}{256}\kappa_5 c^5 + \mathcal{O}(c^7), \tag{2.13}$$

with

$$\kappa_1 := \left(\alpha\hat{\tau} + \beta\frac{\hat{\theta}}{D} - \frac{2\sqrt{2}}{3}\right),\ \kappa_3 := \left(\alpha\hat{\tau}^3 + \beta\frac{\hat{\theta}^3}{D^3}\right),\ \kappa_5 := \left(\alpha\hat{\tau}^5 + \beta\frac{\hat{\theta}^5}{D^5}\right).$$

Lemma 2.5. (Organizing center of the butterfly catastrophe) *Consider the existence condition* (2.13)*. For $\hat{\theta}, \hat{\tau} > 0$, we have that $\Gamma_0(c) = \mathcal{O}(c^5)$ if and only if $\hat{\tau} \neq \hat{\theta}/D$ and*

$$(\gamma, \kappa_1, \kappa_3) = (0, 0, 0),$$

which is is equivalent to

$$(\alpha, \beta, \gamma) = (\alpha_b, \beta_b, 0)$$

where

$$\alpha_b = \left(\frac{2\sqrt{2}}{3}\right)\left(\frac{\hat{\theta}^2}{\hat{\tau}}\right)\left(\frac{1}{\hat{\theta}^2 - \hat{\tau}^2 D^2}\right), \quad \beta_b = -\left(\frac{2\sqrt{2}}{3}\right)\left(\frac{\hat{\tau}^2}{\hat{\theta}}\right)\left(\frac{D^3}{\hat{\theta}^2 - \hat{\tau}^2 D^2}\right). \tag{2.14}$$

There is no parameter constellation such that $\Gamma_0(c) = \mathcal{O}(c^7)$.

Proof. Since $(\alpha, \beta) \mapsto (\kappa_1, \kappa_3)$ is simply an affine transformation, we have that

$$\begin{pmatrix} \kappa_1 \\ \kappa_3 \end{pmatrix} = \begin{pmatrix} 0 \\ 0 \end{pmatrix} = \underbrace{\begin{pmatrix} \hat{\tau} & \widetilde{\theta} \\ \hat{\tau}^3 & \widetilde{\theta}^3 \end{pmatrix}}_{=\mathcal{A}} \begin{pmatrix} \alpha \\ \beta \end{pmatrix} + \begin{pmatrix} -\frac{2\sqrt{2}}{3} \\ 0 \end{pmatrix}$$

$$\Leftrightarrow \begin{pmatrix} \alpha \\ \beta \end{pmatrix} = \begin{pmatrix} \alpha_b \\ \beta_b \end{pmatrix} = \mathcal{A}^{-1}\begin{pmatrix} \frac{2\sqrt{2}}{3} \\ 0 \end{pmatrix} = \left(\frac{1}{\hat{\tau}\widetilde{\theta}\left[\widetilde{\theta}^2 - \hat{\tau}^2\right]}\right)\begin{pmatrix} \widetilde{\theta}^3 & -\widetilde{\theta} \\ -\hat{\tau}^3 & \hat{\tau} \end{pmatrix}\begin{pmatrix} \frac{2\sqrt{2}}{3} \\ 0 \end{pmatrix}$$

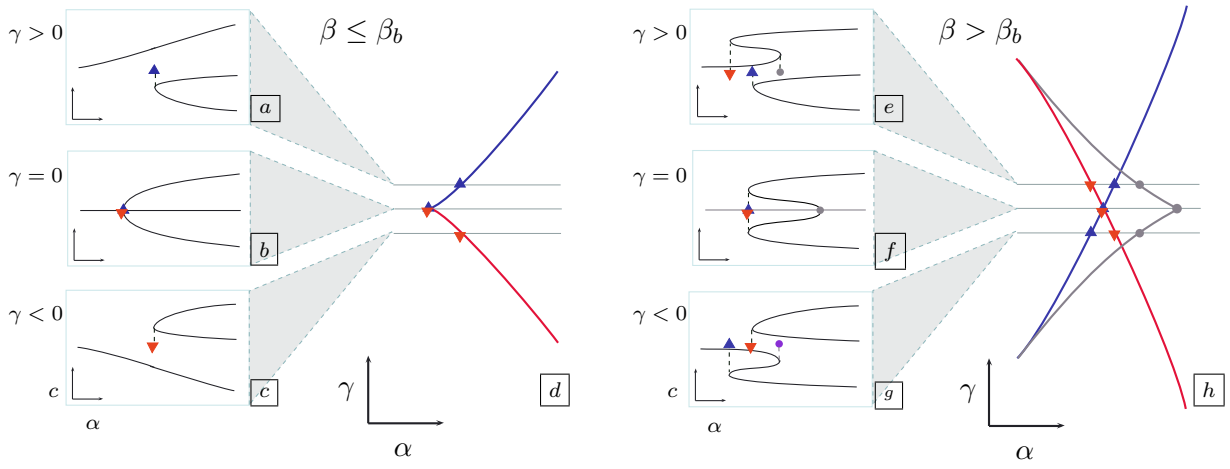

FIGURE 6: Detailed exposition of partially unfolded butterfly catastrophe created by the bifurcation parameters γ, α, β with fixed $\hat{\tau} = 10, \hat{\theta} = 5$ and $D = 2$.

with $\widetilde{\theta} = \frac{\hat{\theta}}{D}$ and where we used that $\det(\mathcal{A}) \neq 0$ if and only if $\hat{\tau} \neq \hat{\theta}/D$ and $\hat{\theta}, \hat{\tau} > 0$. Since

$$\kappa_5(\alpha_b, \beta_b) = -\frac{2\sqrt{2}}{3}\hat{\tau}^2\widetilde{\theta}^2 \neq 0$$

this concludes the proof. □

Directly examining the existence condition (2.10) gives another viewpoint on Lemma 2.5 and the bifurcation scenario in Figure 6. Setting $\gamma = 0$ in (2.10) always yields the solution $c = 0$, which is the only solution if $\hat{\tau} = \hat{\theta} = 0$. In case $\hat{\tau} > 0$ or $\hat{\theta} > 0$, there can be coexisting traveling fronts which can be found, for instance, by examining the dependence $\alpha = \alpha(c)$, that is,

$$\alpha(c) = \frac{\sqrt{c^2\hat{\tau}^2 + 4}}{\hat{\tau}} \left(\frac{\sqrt{2}}{3} - \beta \left(\frac{c\widetilde{\theta}}{\sqrt{c^2\widetilde{\theta}^2 + 4}} \right) \right) \tag{2.15}$$

for fixed $\hat{\tau}$ and $\hat{\theta}$ and varying β (recall $\widetilde{\theta} = \hat{\theta}/D$). At the critical value

$$\frac{d}{dc}\alpha(0) = \frac{1}{\hat{\tau}} \left(\frac{2\sqrt{2}}{3} - \beta\widetilde{\theta} \right) =: \alpha_p\,, \quad \beta \neq \beta_b\,, \tag{2.16}$$

a pitchfork bifurcation occurs (see Figure 6, (b)) which can be super- or subcritical depending on the sign of

$$\frac{d^2}{dc^2}\alpha(0) = \frac{\beta\widetilde{\theta}\left(\widetilde{\theta}^2 - \hat{\tau}^2\right) + 3\sqrt{2}\hat{\tau}^2}{4\hat{\tau}}\,,$$

giving rise to the critical value for β_b in (2.14) which distinguishes these two cases (see Figure 6, (b) and (f)). The value of α at the organizing center is, hence, $\alpha_b = \alpha_p(\beta_b)$. For $\gamma \neq 0$ the reflection symmetry of (1.1) is broken which is reflected in the bifurcation diagrams as imperfect pitchfork bifurcations (see Figure 6, $(a), (c), (e)$ and (g)). The information of the different bifurcation diagrams

is usually distilled into graphs that only keep track of fold locations, which in the case $\beta \leq \beta_b$ leads to the cusp in Figure 6 (d) and otherwise to the butterfly in Figure 6 (h).

Recall that (2.10) really is a leading order existence condition, that is, for $\varepsilon = 0$. Geometric singular perturbation theory combined with the implicit function theorem ensures the persistence of this structure for $\varepsilon > 0$, a fact that we sum up in a corollary for convenience.

Corollary 2.6. *Assume $\hat{\tau} - \hat{\theta}/D = \mathcal{O}(1)$ with respect to ε. For ε sufficiently small, there exists a $\tilde{\beta}_b$, to leading order given by β_b, such that the following holds true.*

(i) If $\beta < \tilde{\beta}_b$, then there exists a parameter combination $(\tilde{\alpha}_p, \tilde{\gamma}_p)$, to leading order given by $(\alpha_p, 0)$, such that the full system undergoes a **supercritical pitchfork** *bifurcation.*

(ii) If $\beta > \tilde{\beta}_b$, then there exists a parameter combination $(\tilde{\alpha}_p, \tilde{\gamma}_p)$, to leading order given by $(\alpha_p, 0)$, such that the full system undergoes a **subcritical pitchfork** *bifurcation.*

(iii) Setting $\gamma = \tilde{\gamma}_p + \check{\gamma}$ with sufficiently small varying $\check{\gamma}$ creates a **partially unfolded butterfly catastrophe**.

Remark 2.7. *The use of α, β, γ as bifurcation parameters is not stringent. Since α and $\hat{\tau}$ (and resp. β and $\hat{\theta}$) appear only as products in* (2.10)*, one can interchange their roles. Furthermore, one could also use β for the pitchfork bifurcation and α to deform it (see Figure 6). Note that, in contrast to the standard bifurcation scenario for the butterfly catastrophe, the cusp point moves as it is being deformed into a butterfly. However, with the affine transformation in the proof of Lemma 2.5 the cusp point is fixed.*

2.3 Special features of the three-component model

Recall that (1.1) is of FitzHugh-Nagumo type, but with an additional third component W. The question arises in which way the third component W enriches the dynamics. One answer is given by the bifurcation analysis of the last section which uncovers that in order to deform the cusp to create the butterfly, we need the parameter β which directly controls the influence of the W-component on the U-component. In other words, the third component increases the complexity of the bifurcation scenario from a cusp to a butterfly (see Figure 6).

However, we only see a partially unfolded butterfly catastrophe. This is due to the symmetries of our system (1.1) which are inherited by the traveling wave ODE (2.1). The fact that our system is autonomous implies the usual reflection symmetry $(c, x) \to (-c, -x)$, such that for any given solution $(u, p, v, q, w, r)(x)$ with velocity parameter c, the function $(u, p, v, q, w, r)(-x)$ is a solution for speed $-c$. Since the vector field together with the parameter γ is odd, (2.1) enjoys the symmetry

$$(c, x, u, p, v, q, w, r, \gamma) \to (c, x, -u, -p, -v, -q, -w, -r, -\gamma)$$

and in combination with the spatial reflection symmetry we obtain

$$(c, x, u, p, v, q, w, r, \gamma) \to (-c, -x, -u, -p, -v, -q, -w, -r, -\gamma).$$

As expected the (leading order) existence condition (2.10) reflects this. Furthermore, noting that fronts at $\gamma = c = 0$ are odd and unique, and thus invariant under $(u, p, v, q, w, r) \to (-u, -p, -v, -q, -w, -r$ one can sum up the symmetry properties of the bifurcation as follows.

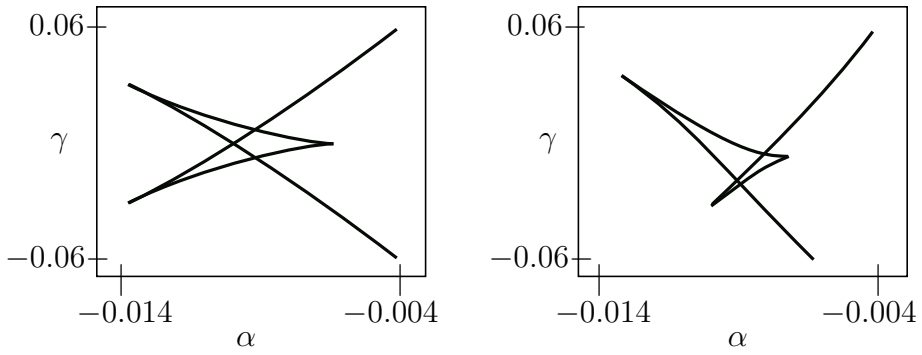

FIGURE 7: The butterfly catastrophe described in Corollary 2.6 and depicted in Fig. 6 is confirmed by the bifurcation software AUTO-07P for the traveling wave ODE (2.1) on an interval of length 50 with Neumann boundary conditions and the integral condition $\int_0^{50} v(x)\,dx = 0$. Parameter setting: $\varepsilon = 0.1, \beta = 0.85, \hat{\theta} = 2, \hat{\tau} = 2, D = 2$. *Left Panel:* Butterfly catastrophe in the (α, γ)-plane. *Right Panel:* Asymmetric butterfly catastrophe for the traveling wave ODE derived from the extended PDE (2.17) with $\mu = 0.002$ in the (α, γ)-plane.

Lemma 2.8. *The image of any solution under the reflection $(c, \gamma) \to (-c, -\gamma)$ is also a solution. In particular, if there is a unique branch bifurcating from $c = \gamma = 0$ as c or γ vary, then it possesses the symmetry.*

This implies that the unfolding by the system parameters is constrained to lie within the symmetry subspace also for the full ε-dependent existence condition, so there are no terms of even power in c at any order in ε. As a result, the butterfly is only partially unfolded. In order to fully unfold the butterfly catastrophe, one could modify our system by adding a quadratic term to the U equation, *e.g.* adding $\varepsilon\mu V^2$ to the U equation which breaks the aforementioned symmetry, that is,

$$\begin{cases} U_t &= U_{\xi\xi} + U - U^3 - \varepsilon(\alpha V + \beta W + \gamma + \mu V^2)\,, \\ \hat{\tau} V_t &= V_{\xi\xi} + \varepsilon^2(U - V)\,, \\ \hat{\theta} W_t &= D^2 W_{\xi\xi} + \varepsilon^2(U - W)\,. \end{cases} \tag{2.17}$$

See the right panel of Figure 7 for an asymmetric butterfly catastrophe obtained from this extended system.

3 Stability of fronts

In the previous section, we have demonstrated the existence of uniformly traveling fronts and now proceed to study their stability. To this end we introduce a co-moving frame by $(x, t) \to (x - \varepsilon^2 ct, t) = (y, t)$, so that (1.1) becomes

$$\begin{cases} \partial_t U &= \varepsilon^2 U_{yy} + \varepsilon^2 c U_y + U - U^3 - \varepsilon(\alpha V + \beta W + \gamma)\,, \\ \hat{\tau}\partial_t V &= \varepsilon^2 V_{yy} + \varepsilon^2 c\hat{\tau} V_y + \varepsilon^2(U - V)\,, \\ \hat{\theta}\partial_t W &= \varepsilon^2 D^2 W_{yy} + \varepsilon^2 c\hat{\theta} W_y + \varepsilon^2(U - W)\,, \end{cases}$$

which upon setting $Z = (U, V, W)$ can be abbreviated as

$$M\partial_t Z = G(Z) + \varepsilon^2 c M \partial_y Z, \quad M = \mathrm{diag}[1, \hat{\tau}, \hat{\theta}]. \tag{3.1}$$

Linearized around Z_{tf} from Proposition 2.2, it reads

$$\begin{cases} \partial_t U &= \left[\varepsilon^2\partial_y^2 + \varepsilon^2 c\partial_y + (1 - 3U_{\mathrm{tf}}^2)\right] U &- \varepsilon(\alpha V + \beta W)\,, \\ \hat{\tau}\partial_t V &= \left[\varepsilon^2\partial_y^2 + \varepsilon^2 c\hat{\tau}\partial_y - \varepsilon^2\right] V &+ \varepsilon^2 U\,, \\ \hat{\theta}\partial_t W &= \left[\varepsilon^2 D^2\partial_y^2 + \varepsilon^2 c\hat{\theta}\partial_y - \varepsilon^2\right] W &+ \varepsilon^2 U\,, \end{cases}$$

which can be abbreviated as

$$M\partial_t Z = \mathbb{L}_c Z, \quad \mathbb{L}_c = \partial_Z G(Z_{\mathrm{tf}}) + \varepsilon^2 c M \partial_y. \tag{3.2}$$

It is standard to split the spectrum $\sigma(\mathbb{L}_c)$ of $\mathbb{L}_c$ into (the disjoint sets) *essential spectrum* $\sigma_{\mathrm{ess}}(\mathbb{L}_c)$ and *point spectrum* $\sigma_{\mathrm{pt}}(\mathbb{L}_c)$ (cf., for instance, [Hen81, Sa02]). The essential spectrum can be computed as in [vHDK08], so we omit the proof here.

Lemma 3.1. (Essential spectrum $\sigma_{\mathrm{ess}}(\mathbb{L}_c)$) *For ε sufficiently small, the essential spectrum of the operator $\mathbb{L}_c$ in* (3.2) *arising from the linearization around a uniformly traveling front Z_{tf} from Proposition 2.2, lies in the open left half plane*

$$\{\lambda \in \mathbb{C} : \mathbb{R}(\lambda) < \lambda_0\}, \quad b < \lambda_0 < 0, \qquad b = \max\left\{-2, -\frac{\varepsilon^2}{\hat{\tau}}, -\frac{\varepsilon^2}{\hat{\theta}}\right\}.$$

The translation symmetry of our system allows to gain some insight into the point spectrum.

Lemma 3.2. (The zero EV of $\mathbb{L}_c$ and Jordan block structure) *Assume a parameter regime where traveling fronts as described in Proposition 2.2 exist.*

(i) The point spectrum $\sigma_{\mathrm{pt}}(\mathbb{L}_c)$ of the operator $\mathbb{L}_c$ always contains zero with corresponding eigenspace containing $\mathrm{span}\{\partial_y Z_{\mathrm{tf}}\}$.

(ii) For $c = 0$, the algebraic multiplicity of the eigenvalue zero at the pitchfork bifurcation value $\widetilde{\alpha}_p$, which to leading order is given by α_p from (2.16)*, is at least two and a generalized eigenfunction ψ is given by*

$$\partial_c Z_{\mathrm{tf}}|_{c=0} =: \psi. \tag{3.3}$$

Proof. The first statement of the lemma follows immediately from the translation invariance of our system (3.1). To prove the second part, we observe that the existence theorem for uniformly traveling fronts, Proposition 2.2, guarantees that for fixed parameters $\beta, \hat{\tau}, \hat{\theta}, D$ and $\gamma = 0$ there is a smooth function $\alpha = \alpha(c)$ (with $\alpha(c) = \widetilde{\alpha}_p$ if and only if $c = 0$) giving rise to a smooth family of uniformly traveling fronts $Z_{\mathrm{tf}} = Z_{\mathrm{tf}}(c)$ which are stationary solutions of the traveling wave PDE (3.1), so

$$0 = G(Z_{\mathrm{tf}}(c)) + \varepsilon^2 c M \partial_y Z_{\mathrm{tf}}(c)\,. \tag{3.4}$$

Taking a derivative w.r.t. c of this relation gives

$$0 = \partial_Z G(Z_{\mathrm{tf}}(c))\partial_c Z_{\mathrm{tf}}(c) + M\partial_y Z_{\mathrm{tf}}(c) + \varepsilon^2 cM\partial_c Z_{\mathrm{tf}}(c)\,.$$

Recall that $\partial_y Z_{\mathrm{tf}}(0) = \partial_x Z_{\mathrm{sf}}$ is an eigenfunction for the zero eigenvalue. Then the above expression evaluated at the pitchfork bifurcation point $c = 0$ gives

$$0 = \partial_Z G(Z_{\mathrm{sf}})\partial_c Z_{\mathrm{tf}}|_{c=0} + M\partial_y Z_{\mathrm{sf}}\,,$$

from which we can readily conclude that $\partial_c Z_{\mathrm{tf}}|_{c=0}$ is a corresponding generalized eigenfunction for $\alpha = \tilde{\alpha}_p$. □

In order to get insight into the nontrivial point spectrum, let us write out the eigenvalue problem in the fast variable $\eta = \frac{y}{\varepsilon}$

$$\begin{cases} \left[\partial_\eta^2 + \left(1 - 3\left(U_{\mathrm{tf}}\right)^2\right)\right] u & - & \varepsilon(\alpha v + \beta w - c u_\eta) & = & \lambda u\,, \\ \left[\partial_\eta^2 + \varepsilon c\hat{\tau}\partial_\eta - \varepsilon^2\right] v & + & \varepsilon^2 u & = & \hat{\tau}\lambda v\,, \\ \left[D^2\partial_\eta^2 + \varepsilon c\hat{\theta}\partial_\eta - \varepsilon^2\right] w & + & \varepsilon^2 u & = & \hat{\theta}\lambda w\,. \end{cases} \tag{3.5}$$

Even though the stability problem inherits the slow/fast-structure of our original system, it is non-autonomous which makes geometric singular perturbation theory less convenient. We refrain from displaying a full rigorous derivation of the point spectrum calculation at this point and instead give some formal arguments that can be made rigorous by Evans function analysis (see Appendix B). In the singular limit $\varepsilon \to 0$ the eigenvalue problem (3.5) reduces to

$$\partial_\eta^2 u + \left(1 - 3\tanh^2\left(\frac{\eta}{\sqrt{2}}\right)\right) u = \lambda u$$

which is known to have eigenvalues $\lambda_0 = 0$ (due to translation symmetry) and $\lambda_{\mathrm{large}} = -\frac{3}{2}$. Hence, we expect for $\varepsilon > 0$ point spectrum close to these values. However, since we are interested in instabilities and bifurcations of fronts, we will focus on point spectrum around 0, which, in the language of [vHDK08], we refer to as *small eigenvalues* (as opposed to the *large eigenvalues* around $-\frac{3}{2}$). It turns out (see Appendix B for details) that there are *small eigenvalues*

$$\lambda = \varepsilon^2\hat{\lambda}$$

of which (again due to translation symmetry) there is always at least one, the eigenvalue $\hat{\lambda}_0 = 0$ (recall Lemma 3.2). Consequently, spectral stability of uniformly traveling fronts is decided by the location of these small eigenvalues. The results are summarized in Lemma 3.3 and Theorem 3.4 (which are proven in Appendix B).

Lemma 3.3. (Point spectrum $\sigma_{\mathrm{pt}}(\mathbb{L}_c)$) *For ε sufficiently small, the point spectrum $\sigma_{\mathrm{pt}}(\mathbb{L}_c)$ of the operator $\mathbb{L}_c$ in* (3.2) *arising from the linearization around a uniformly traveling front Z_{tf} from Proposition 2.2, can be split into two disjoint sets $\sigma_{\mathrm{pt,large}}(\mathbb{L}_c), \sigma_{\mathrm{pt,small}}(\mathbb{L}_c)$. The eigenvalues in $\sigma_{\mathrm{pt,large}}(\mathbb{L}_c)$ are in the open left half-plane, uniformly bounded away from the imaginary axis by an $\mathcal{O}(1)$ (w.r.t. ε) bound. The set $\sigma_{\mathrm{pt,small}}(\mathbb{L}_c)$ contains the eigenvalues that are to leading order in one-to-one correspondence to the roots of the so-called Evans function*

$$E_c(\hat{\lambda}) = -\frac{\sqrt{2}}{6}\hat{\lambda} + \alpha F_{c\hat{\tau},\hat{\tau}}(\hat{\lambda}) + \frac{\beta}{D}F_{c\hat{\theta}/D,\hat{\theta}}(\hat{\lambda})\,, \tag{3.6}$$

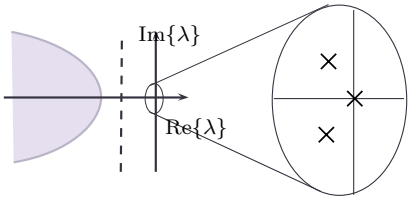

FIGURE 8: Sketch of a possible constellation for $\sigma(\mathbb{L}_c)$. The shaded region illustrates the essential spectrum $\sigma_{\text{ess}}(\mathbb{L}_c)$ and the dashed vertical line indicates its bound as derived in Lemma 3.1. There are at most three small eigenvalues (see zoomed in frame). Recall that both, essential spectrum and small eigenvalues are $\mathcal{O}(\varepsilon^2)$ close to the imaginary axis.

where

$$F_{\rho_1,\rho_2}(\hat{\lambda}) = \left(\frac{1}{\sqrt{\rho_1^2+4}} - \frac{1}{\sqrt{\rho_1^2+4(\hat{\lambda}\rho_2+1)}} \right).$$

Theorem 3.4. (Stability of uniformly traveling fronts) *Assume that the system parameters of* (1.1) *are such that Proposition 2.2 guarantees the existence of a uniformly traveling front* Z_{tf}*. Then for* $\varepsilon > 0$ *sufficiently small this front is stable if the equation* (3.6) *has, apart from the translation invariance solution* $\hat{\lambda}_0 = 0$*, only solutions* $\hat{\lambda}$ *with non-positive real part.*

Remark 3.5. *Note that in [DvHK09] a traveling pulse was constructed by concatenating two fronts separated by a distance that is denoted by* ξ^* *in [DvHK09]. Our existence condition* (2.10) *is consistent with the first existence condition of (3.13) in [DvHK09] in the limit* $\xi^* \to \infty$*. Moreover, for* $c = 0$ *our Evans function* (3.6) *is consistent with the Evans function (5.5) in [vHDK08] again in the limit* $\xi^* \to \infty$*. However, there is no expression in [vHDK08] that allows to find the full Evans function as given in* (3.6)*.*

The proof (in Appendix B) relies essentially on the methods used in [vHDK08] where 2-fronts were studied. Since for a single front the eventful parameter regime of large τ, θ are more amenable to analysis, we can now determine the complete picture of possible bifurcations of stationary and uniformly traveling front solutions. To be more precise, (3.6) allows to conclude the maximal number of small eigenvalues, which is directly related to the possible dimension of the reduced ODE on the center manifold (see Section 4).

Lemma 3.6. (Maximum number of small eigenvalues in $\sigma_{\text{pt}}(\mathbb{L}_c)$**)** *There are at most three small eigenvalues for the operator* $\mathbb{L}_c$ *in* (3.2) *arising from the linearization around a uniformly traveling front from Proposition 2.2.*

Proof. The rather technical proof can be found in Appendix C. □

3.1 Onset of instability for stationary fronts

To study instabilities of stationary fronts, we examine (3.6) for $c = 0$, so

$$2E_0(\hat{\lambda}) =: E(\hat{\lambda}) = \frac{1}{2}\kappa_1\hat{\lambda} + \delta_2\hat{\lambda}^2 + \delta_3\hat{\lambda}^3 + \mathcal{O}(\hat{\lambda}^4), \tag{3.7}$$

where κ_1 is as defined in (2.13), so

$$\kappa_1 = \left(\alpha\hat{\tau} + \frac{\beta}{D}\hat{\theta} - \frac{2\sqrt{2}}{3}\right), \quad \delta_2 := \frac{3}{4}\left(\alpha\hat{\tau}^2 + \frac{\beta}{D}\hat{\theta}^2\right), \quad \delta_3 := \frac{15}{8}\left(\alpha\hat{\tau}^3 + \frac{\beta}{D}\hat{\theta}^3\right).$$

For small $\hat{\tau}$ and $\hat{\theta}$ this expression reduces at leading order to $E(\hat{\lambda}) = -\frac{\sqrt{2}}{3}\hat{\lambda}$, and, hence, zero is the only eigenvalue and local bifurcations occur. From the above expansion (3.7) we can immediately read off when the multiplicity of the zero eigenvalue increases, which paves the way for bifurcations. Elementary computations give the following result.

Lemma 3.7. (Multiplicity of the zero root of the Evans function) *Assume $D > 1$, $\hat{\tau}, \hat{\theta} > 0$ and $\alpha, \beta \in \mathbb{R}\backslash\{0\}$. If $(\alpha, \beta, \hat{\tau}, \hat{\theta}, D)$ are chosen on the surface S defined by*

$$S = \left\{ (\alpha, \beta, \hat{\tau}, \hat{\theta}, D) \in \mathbb{R}^5 \;\middle|\; \kappa_1 = \alpha\hat{\tau} + \frac{\beta}{D}\hat{\theta} - \frac{2\sqrt{2}}{3} = 0 \right\}, \tag{3.8}$$

then E from (3.7) has a double zero root. If, in addition,

$$\delta_2 = \alpha\hat{\tau}^2 + \frac{\beta}{D}\hat{\theta}^2 = 0\,, \tag{3.9}$$

the zero root of E is triple. Combining (3.8) and (3.9) gives

$$(\kappa_1, \delta_2) = (0, 0)\,,$$

or, equivalently,

$$(\alpha, \beta) = (\alpha_{\text{triple}}, \beta_{\text{triple}})\,,$$

where

$$\alpha_{\text{triple}} = -\left(\frac{2\sqrt{2}}{3}\right)\frac{\hat{\theta}}{\hat{\tau}(\hat{\tau} - \hat{\theta})}\,, \quad \frac{\beta_{\text{triple}}}{D} = \left(\frac{2\sqrt{2}}{3}\right)\frac{\hat{\tau}}{\hat{\theta}(\hat{\tau} - \hat{\theta})}\,. \tag{3.10}$$

So, for the triple zero root, α and β have different signs and $\hat{\tau} \neq \hat{\theta}$. The zero root has at most multiplicity three.

As a consequence of Lemma 3.7 and the construction via geometric singular perturbation theory the following holds true for the possible algebraic multiplicity of the zero eigenvalue of the operator $\sigma_{\text{pt}}(\mathbb{L}_0)$.

Corollary 3.8. (Multiplicity of the zero eigenvalue in $\sigma_{\text{pt}}(\mathbb{L}_0)$) *Let the conditions in Lemma 3.7 be fulfilled. In an $\mathcal{O}(\varepsilon)$-neighborhood of the parameter combination resulting in a double (resp. triple) root of the Evans function there is a corresponding parameter combination for which the operator $\sigma_{\text{pt}}(\mathbb{L}_0)$ has an algebraically double (resp. triple) zero eigenvalue.*

Further elementary computations (combining the parameter regimes in Lemma 2.6 and Lemma 3.7) indicate the possibility of a Bogdanov-Takens bifurcation scenario with butterfly imprint.

Lemma 3.9. (Butterfly catastrophe and triple zero eigenvalue) *The organizing center of the butterfly catastrophe in Lemma 2.5 coincides with a triple zero eigenvalue if*

$$(\gamma, \kappa_1, \kappa_3, \delta_2) = (0, 0, 0, 0)\,,$$

or, equivalently,

$$(\gamma, \alpha, \beta, D) = (0, \alpha_{\mathrm{b,tr}}, \beta_{\mathrm{b,tr}}, D_{\mathrm{b,tr}})\,,$$

where

$$\alpha_{\mathrm{b,tr}} = -\frac{2\sqrt{2}}{3}\frac{\hat\theta}{\hat\tau(\hat\tau-\hat\theta)}\,, \quad \beta_{\mathrm{b,tr}} = \frac{2\sqrt{2}}{3}\frac{\sqrt{\hat\tau}}{\sqrt{\hat\theta}(\hat\tau-\hat\theta)}\,, \quad D_{\mathrm{b,tr}} = \sqrt{\frac{\hat\theta}{\hat\tau}}\,.$$

Since $D > 1$ we need $\hat\theta > \hat\tau$.

3.2 Pitchfork bifurcation of a stationary front

Parameter regimes around the double zero eigenvalue are expected to give rise to a pitchfork bifurcation. In the next section, we will examine the pitchfork bifurcation for stationary fronts (so $c = 0$) by center manifold reduction. To facilitate the exposition, we will restrict the discussion to the case $\hat\tau = \hat\theta = 1$, where we have explicit control over the roots.

Lemma 3.10. *Consider the roots of E_c from (3.6) for $c = 0, \hat\tau = \hat\theta = 1$.*

(i) If $\alpha + \beta/D \le 0$, the zero root is simple, while the real part of a possible complex conjugate pair is less than $-\frac{3}{4}$.

(ii) If $\alpha + \beta/D > 0$, there are exactly two roots and both roots are real.

(iii) There is an open neighborhood $U_c \in \mathbb{R}$ of $\alpha_p = \frac{2\sqrt{2}}{3} - \beta/D$, such that for $\alpha \in U_c$ we have exactly two roots and both are real.

Remark 3.11. *Note that the condition $\hat\tau = \hat\theta = 1$ excludes the possibility of having a triple zero eigenvalue, but allows the butterfly catastrophe since this requires $\hat\tau \neq \frac{\hat\theta}{D}$ and $D > 1$ by assumption.*

Proof. The Evans function E in (3.6) with $c = 0, \hat\tau = \hat\theta = 1$ has at most three roots by elementary considerations. If $\alpha + \beta/D \le 0$, then

$$f(\hat\lambda) = g(\hat\lambda)$$

with

$$f(\hat\lambda) := -\frac{\sqrt{2}}{3}\hat\lambda + \alpha + \beta/D\,, \qquad g(\hat\lambda) := \frac{\alpha + \beta/D}{\sqrt{\hat\tau\hat\lambda + 1}}\,, \tag{3.11}$$

has only $\hat\lambda = 0$ as solution (see panel (a) of Figure 9) and inspection of the explicit expressions for the roots of the third order polynomial shows that, if there are complex roots, their real part is always bounded from above by $-\frac{3}{4}$. So, *(i)* follows. Similarly, if $\alpha + \beta/D > 0$, there are exactly two crossing points of f and g (see panels (b)-(e) of Figure 9), which excludes the existence of a third eigenvalue, so, *(ii)* follows. Lastly, for $\alpha = \alpha_p + \check\alpha$ we have $\alpha + \beta/D = \frac{2\sqrt{2}}{3} + \check\alpha > 0$ for $\check\alpha$ small enough, so, by (ii), we have exactly two roots and both are real, which shows *(iii)*. □

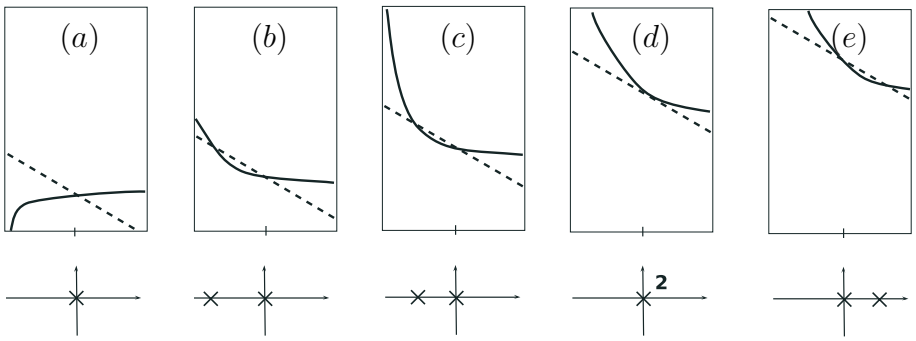

FIGURE 9: Illustration of the crossing of the functions f (solid) and g (dashed) from (3.11) for and corresponding eigenvalues for $(a) : \alpha + \beta/D = -0.1$, $(b) : \alpha + \beta/D = 0.1$, $(c) : \alpha + \beta/D = \frac{2\sqrt{2}}{3} - 0.6$, $(d) : \alpha + \beta/D = \frac{2\sqrt{2}}{3}$, $(e) : \alpha + \beta/D = \frac{2\sqrt{2}}{3} + 1$

Again, the pitchfork bifurcation described in the previous lemma persists for $\varepsilon > 0$ and coincides with the bifurcation described in Corollary 2.6. In order to prepare the center manifold reduction in Section 4 we summarize the spectral features of the operator $\sigma_{\mathrm{pt}}(\mathbb{L}_0)$:

Lemma 3.12. (Eigenspace and spectral projections for the double zero of $\sigma_{\mathrm{pt}}(\mathbb{L}_0)$) *Fix $\gamma = 0, \hat{\tau} = \hat{\theta} = 1$ and $\varepsilon > 0$ sufficiently small.*

(i) There is $\widetilde{\alpha}_p$ (to first order given by α_p from Lemma 3.10) such that the operator $\mathbb{L}_0(\widetilde{\alpha}_p)$ in (3.2) with $c = 0$ arising from the linearization around a stationary front Z_{sf} from Proposition 2.2 has a zero eigenvalue with algebraic multiplicity one and geometric multiplicity two. In more detail, we have

$$\mathbb{L}_0(\widetilde{\alpha}_p)\phi = 0, \quad \phi = Z'_{\mathrm{sf}}, \qquad \mathbb{L}_0(\widetilde{\alpha}_p)\psi = \phi, \quad \psi = \partial_c Z_{\mathrm{tf}}|_{c=0}\,. \tag{3.12}$$

Setting $\alpha = \widetilde{\alpha}_p + \check{\alpha}$ for sufficiently small $\check{\alpha}$ creates a pitchfork bifurcation. Furthermore, introducing the phase space $\chi = H^s(\mathbb{R})^3, s \geq 2$, (product space of L^2-based Sobolev spaces) and the duality product

$$\langle Z, \widetilde{Z}\rangle_\chi = \langle U, \widetilde{U}\rangle_{L^2} + \langle V, \widetilde{V}\rangle_{L^2} + \langle W, \widetilde{W}\rangle_{L^2}\,, \tag{3.13}$$

we know that for the adjoint operator $\mathbb{L}_0^*$ we have the corresponding properties, so

$$\mathbb{L}_0^*(\widetilde{\alpha}_p)\phi^* = 0, \qquad \mathbb{L}_0^*(\widetilde{\alpha}_p)\psi^* = \phi^*\,. \tag{3.14}$$

(ii) The functions $\phi, \phi^*, \psi, \psi^*$ define a projection onto the spectral subspace $E_0 = \mathrm{span}[\phi, \psi]$ (belonging to the zero eigenvalue) by

$$\mathbb{P}_{E_0}\{\cdot\} = \langle \cdot, \psi^*\rangle_\chi \phi + \langle \cdot, \phi^*\rangle_\chi \psi. \tag{3.15}$$

We have $\langle \phi, \phi^*\rangle_\chi = 0$ and we can choose the functions such that $\langle \phi, \psi^*\rangle_\chi = \langle \phi^*, \psi\rangle_\chi = 1$ and $\langle \psi, \psi^*\rangle_\chi = 0$. Furthermore, define $\mathbb{P}_{E_-} = \mathrm{Id} - \mathbb{P}_{E_0}$, so $E_- = R(\mathbb{P}_{E_-})$ is the spectral subspace belonging to $\sigma_- := \sigma(\mathbb{L}_0) \setminus \{0\}$. In other words, we have the splitting

$$\chi = E_0 \oplus E_-\,.$$

(iii) The functions $\phi, \phi^*, \psi, \psi^*$ are all even.

Proof. Parts (i) and (ii) are a combination of restating Lemma 3.2, using geometric singular perturbation theory to argue the persistence of the leading order result in Lemma 3.10 and basic spectral theory. The parity of the eigenfunctions stated in (iii) can be understood from the following argument: The front solution Z_{sf} is odd, so $\phi = Z_{\mathrm{sf}}'$ is even. The operator $\mathbb{L}_0$ is of second order and features multiplication with an even function, and, hence, preserves parity. □

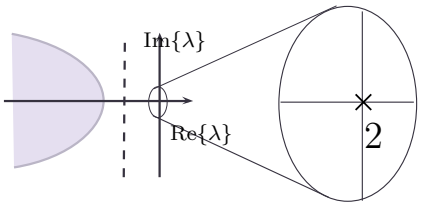

FIGURE 10: Double zero eigenvalue for $\sigma(\mathbb{L}_0)$. The shaded region illustrates the essential spectrum, the striped vertical line its bound and the cross the large eigenvalue $\tilde{\lambda}_{\mathrm{large}}$.

4 Dynamics of bifurcating front solutions

In this section, we perform a center manifold reduction to unfold the butterfly catastrophe from Section 2.2 by making use of the spectral properties of the operator $\mathbb{L}_0$ (see Lemma 3.12). This will result in a reduced equation describing dynamically evolving fronts that bifurcate from stationary ones.

Let us write our system (1.1) in the more compact form

$$\partial_t Z = G(Z)\,. \tag{4.1}$$

In the realm of center manifold reduction for systems with continuous symmetries we set

$$Z(\cdot,t) = T_{a(t)}[Z_{\mathrm{sf}}(\cdot) + \bar{R}(\cdot,t)] = T_{a(t)}[Z_{\mathrm{sf}}(\cdot) + b(t)\psi(\cdot) + R(\cdot,t)]\,, \tag{4.2}$$

where T_a is the translation operator $T_a(f)(\cdot) = f(\cdot - a)$, ψ is a generalized eigenfunction (cf. Lemma 3.12) and $a, b, R, \bar{R}$ are real-valued functions. Note that the coordinate function a on the center manifold describes the position of the front, so $\dot{a}$ is its velocity.

Theorem 4.1. (Velocity of bifurcating fronts) *Fix $\hat{\tau} = \hat{\theta} = 1$ and $\varepsilon > 0$ small enough such that there exists a stationary front Z_{sf} as in Proposition 2.2. For small enough $\check{\alpha}, \check{\beta}, \check{\gamma}$ consider the parameter regime*

$$\alpha = \widetilde{\alpha}_b + \check{\alpha}, \quad \beta = \widetilde{\beta}_b + \check{\beta}, \quad \gamma = \widetilde{\gamma}_b + \check{\gamma}\,,$$

where the critical values $(\tilde{\alpha}_b, \tilde{\beta}_b, \tilde{\gamma}_b)$ are as in Corollary 2.6. Then the velocity $\dot{a}(t) =: \nu(t)$ of a front bifurcating from Z_{sf} satisfies the first order ODE

$$\dot{\nu} = \varepsilon^2 \left[\gamma + \frac{1}{2}\kappa_1\nu + \frac{1}{16}\kappa_3\nu^3 + \frac{3}{256}\kappa_5\nu^5\right] + \text{h.o.t.}\,, \tag{4.3}$$

where $\kappa_1, \kappa_3, \kappa_5$ are defined in (2.13) *and* h.o.t. *denotes higher order terms. In particular, the bifurcation structure of this ODE features a butterfly catastrophe as described in Corollary 2.6.*

Remark 4.2. *We set $\hat{\tau} = \hat{\theta} = 1$ in the upcoming analysis to facilitate the exposition, but would like to stress that this is by no means necessary. Any parameter regime where the third eigenvalue is known to stay in the left half plane will yield the same result.*

Proof. Implementing ansatz (4.2) into the left hand side of (4.1) gives

$$\partial_t Z = \dot{a}(Z_{\mathrm{sf}})' + \dot{b}\psi + \dot{a}b\psi' + \dot{a}\partial_y R + \partial_t R = \dot{a}\phi + \dot{b}\psi + \dot{a}b\psi' + \dot{a}\partial_y R + \partial_t R\,,$$

where $\dot{} = \frac{d}{dt}$ represents a time derivative, while $' = \frac{d}{dy}$ and ∂_y are spatial derivatives w.r.t. $y = x - a(t)$. The right hand side of (4.1) becomes

$$G(Z) = G(Z_{\mathrm{sf}}) + \partial_Z G(Z_{\mathrm{sf}})\bar{R} + \frac{1}{2}\partial_Z^2 G(Z_{\mathrm{sf}})[\bar{R},\bar{R}] + \frac{1}{6}\partial_Z^3 G(Z_{\mathrm{sf}})[\bar{R},\bar{R},\bar{R}],$$

where the residual term $G(Z_{\mathrm{sf}}) = G(Z_{\mathrm{sf}};\check{\gamma}) = (-\varepsilon\check{\gamma},0,0)^t$ accounts for the fact that Z_{sf} is not a solution for non-zero $\check{\gamma}$ and the nonlinear terms are given by

$$\frac{1}{2}\partial_Z^2 G(Z_{\mathrm{sf}})[\bar{R},\bar{R}] + \frac{1}{6}\partial_Z^3 G(Z_{\mathrm{sf}})[\bar{R},\bar{R},\bar{R}] = -(3Z_U^{\mathrm{sf}}(\bar{R}_U)^2 + (\bar{R}_U)^3, 0, 0)^t\,.$$

Note that the expansion is exact since the nonlinearity is a cubic polynomial. In order to use center manifold theory to study the bifurcation we introduce the splitting

$$\partial_Z G(Z_{\mathrm{sf}};\alpha) = \partial_Z G(Z_{\mathrm{sf}};\widetilde{\alpha}_b + \check{\alpha}) = \partial_Z G(Z_{\mathrm{sf}};\widetilde{\alpha}_b) + \underbrace{[\partial_Z G(Z_{\mathrm{sf}};\widetilde{\alpha}_b + \check{\alpha}) - \partial_Z G(Z_{\mathrm{sf}};\widetilde{\alpha}_b)]}_{=:\mathcal{G}(Z_{\mathrm{sf}};\check{\alpha})}$$

where in fact

$$\mathcal{G}(Z_{\mathrm{sf}};\check{\alpha})\bar{R} = -(\varepsilon\check{\alpha}\bar{R}_V, 0, 0)^t.$$

Note, that $Z_{\mathrm{sf}} = Z_{\mathrm{sf}}(\widetilde{\alpha}_b)$ is chosen fixed. Using the above notation we see that the right hand side of (4.1) has the form

$$G(Z;\alpha,\gamma) = \partial_Z G(Z_{\mathrm{sf}};\widetilde{\alpha}_b)\bar{R} + \mathcal{F}(\check{\alpha},\check{\gamma})[\bar{R}]$$

with

$$\mathcal{F}(\check{\alpha},\check{\gamma})[\bar{R}] = (-(\varepsilon\check{\gamma} + \varepsilon\check{\alpha}\bar{R}_V + 3U_{\mathrm{sf}}(\bar{R}_U)^2 + (\bar{R}_U)^3), 0, 0)^t. \tag{4.4}$$

Note that $\mathcal{F}$ has only a U-component. In summary, ansatz (4.2) transforms equation (4.1) into

$$\dot{a}\phi + \dot{b}\psi + \dot{a}b\psi' + \dot{a}\partial_y R + \partial_t R = \partial_Z G(Z_{\mathrm{sf}};\widetilde{\alpha}_b)R - b\phi + \mathcal{F}[b\psi + R]\,. \tag{4.5}$$

We now make use of the properties of the adjoint operator $\mathbb{L}_0^*(\widetilde{\alpha}_b) = \partial_Z G(Z_{\mathrm{sf}};\widetilde{\alpha}_b)^*$ described in Lemma 3.12 and the spectral projections defined therein. Projecting equation (4.5) onto the center eigenspace E_0 and its complement E_- respectively and using the symmetry of eigenfunctions described in Lemma 3.12, part (iii), gives the following coupled ODE-PDE system for (a,b,R):

$$\dot{a} = \frac{1}{s}\left(\frac{1}{s + \langle\partial_y R,\psi^*\rangle}\right)(-sb + \langle\mathcal{F}[b\psi + R],\psi^*\rangle) =: g_a(b,R,\check{\alpha},\check{\gamma})\,, \tag{4.6}$$

$$\dot{b} = \frac{1}{s}\langle\mathcal{F}[b\psi + R],\phi^*\rangle - \frac{1}{s}g_a(b,R,\check{\alpha},\check{\gamma})\langle\partial_y R,\phi^*\rangle\,, \tag{4.7}$$

$$\partial_t R = \mathbb{L}_0(\widetilde{\alpha}_b)R + \mathbb{P}_{E_-}\{\mathcal{F}[b\psi + R] - g_a(b,R,\check{\alpha},\check{\gamma})b\psi' - g_a(b,R,\check{\alpha},\check{\gamma})\partial_y R\}\,. \tag{4.8}$$

Note that, due to the special form of our ansatz, the right hand side of (4.6)-(4.8) does not depend explicitly on a. It is, hence, sufficient to study the subsystem (4.7)-(4.8) for (b, r), since the equation for a can simply be integrated upon knowledge of b and R. The existence of a center manifold for (4.7)-(4.8) that captures all bifurcating solutions follows from standard results (see *e.g.* [HI11], Theorem 3.23), since (4.7)-(4.8) is a semilinear, parabolic problem in a Hilbert space. We state the respective result without proof.

Proposition 4.3. (Center manifold reduction) *Let the parameter regime be as stipulated in Theorem 4.1. Then there is a map $h \in C^k(E_0 \times \mathbb{R}^3, E_-)$ satisfying $h(0) = 0, Dh(0) = 0$ and a neighborhood $\mathcal{U}_{(a,b,R)} \times \mathcal{U}_{(\check{\alpha},\check{\beta},\check{\gamma})} \in H^s(\mathbb{R})^3 \times \mathbb{R}^3$ such that for $(\check{\alpha}, \check{\beta}, \check{\gamma}) \in \mathcal{U}_{(\check{\alpha},\check{\beta},\check{\gamma})}$ the manifold $\{T_a[Z_{\mathrm{sf}} + b\psi + h(b, \check{\alpha}, \check{\beta}, \check{\gamma})]\}$ is locally invariant under the flow of (4.7)-(4.8) and exponentially attracting. Furthermore, it contains the set of all bounded solutions that stay in $\mathcal{U}_{(a,b,R)}$ for all $t \in \mathbb{R}$.*

Note that from (4.6), it is easy to see that $\dot{a} = -b + \mathcal{O}(b^2)$, so the front velocity $\dot{a}(t) = \nu(t)$ will be governed by a scalar ODE. From the existence condition for uniformly traveling fronts, we know the fixed point structure of the evolution equation for the velocity to leading order in ε. Hence, up to a scaling constant δ, the Taylor expansion of the RHS of the ODE coincides with the Taylor expansion of the existence condition (2.13). Using the eigenvalue information from the stability analysis in the last section, we get $\delta = \varepsilon^2$. This concludes the proof of Theorem 4.1.

□

5 Summary and future investigations

We presented the analysis of existence, stability and bifurcations for single, uniformly traveling front solutions in the (FitzHugh-Nagumo type) three-component reaction-diffusion system (1.1) featuring parameters such that the essential spectrum of (the linearization around) stationary fronts is asymptotically close to the origin. By means of geometric singular perturbation theory we were able to give implicit (leading order) expressions for the existence of uniformly traveling fronts (see (2.10)) and their stability (see (3.6)). While the existence analysis follows the approach in [DvHK09] very closely and essentially relies on a Melnikov type argument, the stability analysis – though similar in spirit to [vHDK08] – had to be significantly modified and extended to incorporate parameter regimes where τ and θ are large. We found that there exist at most three small eigenvalues which could lead to instabilities (of which one is always zero due to translational symmetry of the problem). In fact, it turned out that there are parameter regimes for which the multiplicity of the zero eigenvalue is either two or three, providing an entry point for the analysis of bifurcating, dynamically evolving fronts. In our bifurcation analysis we mainly focused on the unfolding of the double zero eigenvalue case for stationary fronts (see Lemma 3.12). By center manifold reduction for equivariant systems, we derived the scalar ODE (4.3) describing the time evolution of the velocity of bifurcating fronts. This ODE bears the imprint of a partially unfolded butterfly (as described in Section 2.2).

More generally, our analysis shows that one may expect to observe the full dynamics of a two-dimensional system near the triple zero point. In particular, it predicts a Bogdanov-Takens type bifurcation scenario with butterfly imprint (see Lemma 3.9). The unfolding of the triple zero eigenvalue case will be the subject of future investigations. Note that a Bogdanov-Takens scenario, for instance, indicates the presence of a Hopf bifurcation near this regime, which we could confirm

numerically (see Figure 11 for an oscillating front solution).

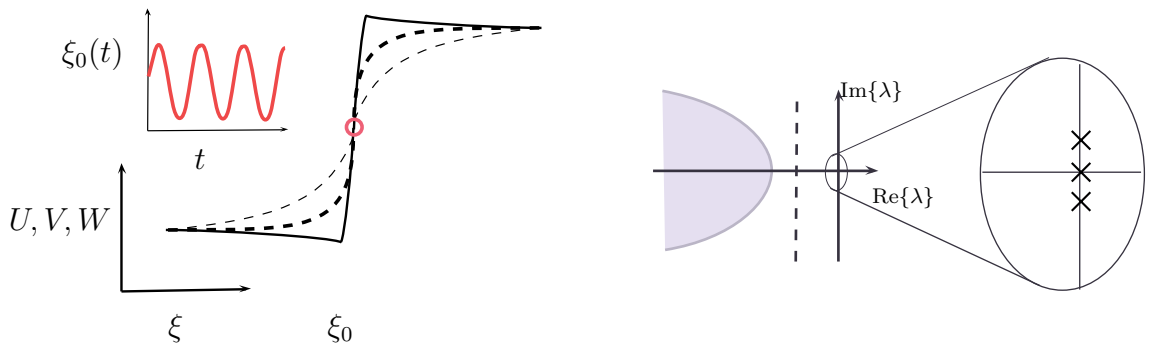

FIGURE 11: Hopf bifurcation leading to an oscillating front. *Left panel*: Spatial profile of a front solution with U solid and V, W dashed (*large plot*) and trajectory of the oscillating front represented by the space-time plot of the zero-crossing ξ_0 of the U-component (*small plot*). *Right panel*: Complex conjugate pair crosses the imaginary axis in the parameter regime of numerically observed oscillations. *Parameter setting*: $\varepsilon = 0.03, \gamma = 0, D = 3, \hat{\tau} = 4.21, \hat{\theta} = 10, \alpha = 0.79, \beta = -1.2057$.

Finally, we return to our original motivation to study system (1.1) with asymptotically large parameters τ and/or θ of order $\mathcal{O}(1/\varepsilon^2)$. In this parameter regime, numerical simulations show very rich front interaction dynamics that are much more complex than for smaller values of τ and θ – see [NTU03, NTYU07, DvHK09]. In [vHDKP10], the validity and local attractivity of an explicitly determined N-dimensional system describing the semi-strong interactions of N fronts has been rigorously established for $\tau, \theta = \mathcal{O}(1)$. Although the dynamics exhibited by these systems are certainly nontrivial – see [vHDKP10] – these systems are intrinsically not capable of describing the front interaction dynamics for large τ and θ. For instance, these systems have a gradient structure and thus cannot describe the periodic behavior observed in the simulations with τ and θ large.

The findings of this paper show that even the dynamics of single fronts – the building blocks of the front interaction dynamics – increase dramatically when τ and/or θ are increased: as Figure 11 shows, solitary fronts may start to oscillate by internal mechanisms, without being in interaction with neighboring fronts (as is the case for the breathing pulses/double fronts studied in [vHDK08]). Thus, the present analysis provides an important element of a further analytical understanding of semi-strong front dynamics. Our analysis strongly indicates that for τ and θ large, the dynamics of a localized front should be described by the 'eigenmodes' associated to the *small eigenvalues* relevant for bifurcations of which there are at most three. In the case $\tau, \theta = \mathcal{O}(1)$, there is only one such eigenfunction, the (spatial) derivative of the front solution associated to the translational invariance of (1.1). As a consequence, the dynamics of N interacting fronts are for $\tau, \theta = \mathcal{O}(1)$ described by an N-dimensional system for the N translational eigenmodes associated to each of the N fronts [vHDKP10]. Our present results, thus, foreshadow that a $3N$-dimensional system might be necessary to describe the interactions of N-fronts when τ, θ become large (in the sense $\tau, \theta = \mathcal{O}(1/\varepsilon^2)$). However, it is not clear yet whether this will be sufficient: from an asymptotic point of view, the impact of the essential spectrum is in principle as strong as that of the point spectrum since they are both of order $\mathcal{O}(\varepsilon^2)$. In fact, the essential spectrum very likely already does play a significant role 'in the background': each of the two additional eigenvalues/eigenmodes (per front) originates from

the essential spectrum as τ, θ increases from $\mathcal{O}(1)$ to $\mathcal{O}(1/\varepsilon^2)$. In other words, the essential spectrum enabled the growth from the N-dimensional front interaction system to a $3N$-dimensional one.

The central question, that will be the topic of future research, is thus: Can the semi-strong N-front dynamics indeed be described by only a $3N$-dimensional system (for $\tau, \theta = \mathcal{O}(1/\varepsilon^2)$)? Both possible answers generate fundamental questions. If the full PDE dynamics differ from that of the $3N$-dimensional system spanned by the localized eigenmodes, then one needs to devise novel methods by which the influence of the essential spectrum can be determined. Even if this is not the case, or if it is not obvious, one needs to go beyond the renormalization group method developed in [DKP07, vHDKP10, BDKP13] to rigorously establish the validity and local attractivity of the $3N$-dimensional dynamics.

A Higher order corrections of the front profile

The stability analysis for uniformly traveling fronts $Z_{\rm tf} = (U_{\rm tf}, V_{\rm tf}, W_{\rm tf})$ as derived in Proposition 2.2 makes use of information about the higher order terms of the front profile (2.3). To ease notation we introduce the abbreviation

$$\sqrt{2}(U^0_{\rm tf})_\eta = \operatorname{sech}^2\left(\frac{\eta}{\sqrt{2}}\right) =: \rho(\eta)\,. \tag{A.1}$$

Upon working in a (fast) co-moving frame $\eta = \xi - \varepsilon c t$ and using a regular expansion for $U_{\rm tf}(\eta)$, that is, $U_{\rm tf}(\eta) = U^0_{\rm tf}(\eta) + \varepsilon U^1_{\rm tf}(\eta) + \varepsilon^2 U^2_{\rm tf}(\eta) + \mathcal{O}(\varepsilon^3)$, with $U^0_{\rm tf}(\eta) = \tanh\left(\frac{\eta}{\sqrt{2}}\right)$, we obtain the following result.

Lemma A.1. *Let the conditions in Proposition 2.2 be fulfilled.*

(i) *The higher correction term $U^1_{\rm tf}(\eta)$ is an even function in the fast field $I_{\rm f}$ (see (2.7)).*

(ii) *Its derivative obeys the relation*

$$\mathcal{L}(U^1_{\rm tf})_\eta := ((U^1_{\rm tf})_\eta)_{\eta\eta} + (U^1_{\rm tf})_\eta - 3(U^0_{\rm tf})^2(U^1_{\rm tf})_\eta = -c(U^0_{\rm tf})_{\eta\eta} + 6U^0_{\rm tf}(U^0_{\rm tf})_\eta U^1_{\rm tf} = -\frac{c}{\sqrt{2}}\rho_\eta + 3\sqrt{2}U^0_{\rm tf}U^1_{\rm tf}\rho\,.$$

(iii) *The next order correction term $U^2_{\rm tf}(\eta)$ obeys the integral relation*

$$\begin{aligned} c\int (U^1_{\rm tf})_{\eta\eta}\rho d\eta - 6\int U^0_{\rm tf}(U^0_{\rm tf})_\eta U^2_{\rm tf}\rho d\eta - 6\int U^0_{\rm tf}U^1_{\rm tf}(U^1_{\rm tf})_\eta\rho d\eta - 3\int (U^0_{\rm tf})_\eta (U^1_{\rm tf})^2\rho d\eta \\ = c\int (U^1_{\rm tf})_{\eta\eta}\rho d\eta - 3\sqrt{2}\int U^0_{\rm tf}U^2_{\rm tf}\rho^2 d\eta - 6\int U^0_{\rm tf}U^1_{\rm tf}(U^1_{\rm tf})_\eta\rho d\eta - \frac{3}{\sqrt{2}}\int (U^1_{\rm tf})^2\rho^2 d\eta \\ = 4\sqrt{2}\left(\alpha\left(\frac{1}{\sqrt{c^2\hat\tau^2+4}}\right) + \frac{\beta}{D}\left(\frac{1}{\sqrt{\frac{c^2\hat\theta^2}{D^2}+4}}\right)\right)\,. \end{aligned}$$

Proof. The proof of this lemma is completely analogues to the proofs in §2.2 of [vHDK08] upon plugging in the correct expressions for the derivatives of the slow components in the fast field $I_{\rm f}$ (from (2.7)). The parity of $U^1_{\rm tf}(\eta)$ follows from expanding $U_{\rm tf}(\eta)$ in a regular fashion and studying

the $\mathcal{O}(\varepsilon)$-level of the U-equation of (3.1). After plugging in the derived existence condition (2.10), we obtain the following equation for $U_{\rm tf}^1$

$$\mathcal{L}U_{\rm tf}^1 = c\left(\frac{\sqrt{2}}{3} - (U_{\rm tf}^0)_\eta\right) = \sqrt{2}c\left(\frac{1}{3} - \frac{1}{2}\rho\right).$$

Since the operator $\mathcal{L}$ conserves parity and the right hand side of the above equation is even, we obtain that $U_{\rm tf}^1(\eta)$ is an even function. The relations for $(U_{\rm tf}^1)_\eta$ and $U_{\rm tf}^2$ follow from studying the derivative of the U-equation of (3.1) in the fast field in the co-moving frame:

$$U_{\eta\eta\eta} = -U_\eta + 3U^2U_\eta + \varepsilon(\alpha V_\eta + \beta W_\eta - cU_{\eta\eta}).$$

After plugging in the regular expansion for $U_{\rm tf}$ and noting that V_η and W_η are $\mathcal{O}(\varepsilon)$ and constant in the fast field, we obtain

$$\begin{aligned}
\mathcal{O}(1) : \mathcal{L}(U_{\rm tf}^0)_\eta =& 0\,,\\
\mathcal{O}(\varepsilon) : \mathcal{L}(U_{\rm tf}^1)_\eta =& -c(U_{\rm tf}^0)_{\eta\eta} + 6U_{\rm tf}^0(U_{\rm tf}^0)_\eta U_{\rm tf}^1\,,\\
\mathcal{O}(\varepsilon^2) : \mathcal{L}(U_{\rm tf}^2)_\eta =& \alpha V_\eta + \beta W_\eta - c(U_{\rm tf}^1)_{\eta\eta} + 6U_{\rm tf}^0(U_{\rm tf}^0)_\eta U_{\rm tf}^2 + 6U_{\rm tf}^0U_{\rm tf}^1(U_{\rm tf}^1)_\eta + 3(U_{\rm tf}^0)_\eta(U_{\rm tf}^1)^2\,,
\end{aligned}$$

where we indicated the correct asymptotic scaling of the slow components by taking their derivatives with respect to the slow variable. To obtain the integral relation involving $U_{\rm tf}^2$, we note that ρ is in the kernel of $\mathcal{L}$ and we apply a solvability condition on the $\mathcal{O}(\varepsilon^2)$-equation. This gives

$$2\sqrt{2}(\alpha V_\eta + \beta W_\eta) = c\int (U_{\rm tf}^1)_{\eta\eta}\rho d\eta - 6\int U_{\rm tf}^0(U_{\rm tf}^0)_\eta U_{\rm tf}^2\rho d\eta - 6\int U_{\rm tf}^0U_{\rm tf}^1(U_{\rm tf}^1)_\eta\rho d\eta - 3\int (U_{\rm tf}^0)_\eta(U_{\rm tf}^1)^2\rho d\eta\,,$$

where we used that $\int \rho(\eta)dt = 2\sqrt{2}$. Finally, from (2.8) we get that

$$\begin{aligned}
V_\eta = \lambda_v^+(v_* + 1) &= \frac{1}{2}\left(-\frac{c^2\hat{\tau}^2}{\sqrt{c^2\hat{\tau}^2+4}} + \sqrt{c^2\hat{\tau}^2+4}\right) = \frac{2}{\sqrt{c^2\hat{\tau}^2+4}}\,,\\
W_\eta = \lambda_w^+(w_* + 1) &= \frac{1}{2}\frac{1}{D}\left(-\frac{\frac{c^2\hat{\theta}^2}{D^2}}{\sqrt{\frac{c^2\hat{\theta}^2}{D^2}+4}} + \sqrt{\frac{c^2\hat{\theta}^2}{D^2}+4}\right) = \frac{1}{D}\left(\frac{2}{\sqrt{\frac{c^2\hat{\theta}^2}{D^2}+4}}\right).
\end{aligned}$$

This completes the proof. □

B Proof of Theorem 3.4 via Evans function analysis

As alluded to, we will make use of the Evans function to compute the point spectrum of our operator. For slow-fast systems, as analyzed in this paper, it has been shown in [AGJ90] that the Evans function $\mathcal{D}(\lambda)$ can be split into an analytic fast part $\mathcal{D}_{\rm f}(\lambda)$ and a meromorphic slow part $\mathcal{D}_{\rm s}(\lambda)$ and a nonzero function $d(\lambda)$. In [DGK98, DGK01, DGK02], the NLEP-method was developed in context of two-component singularly perturbed reaction-diffusion equations by which these two parts of the Evans function can be explicitly computed. In [vHDK08], this method was extended to N-component singularly perturbed reaction-diffusion equations with one fast and $(N-1)$-slow components. In more detail, for $N = 3$ we can write the Evans function $\mathcal{D}(\lambda)$ as

$$\mathcal{D}(\lambda) = d(\lambda)\mathcal{D}_{\rm f}(\lambda)\mathcal{D}_{\rm s}(\lambda) = d(\lambda)t_1^+(\lambda)\left(t_{22}^+(\lambda)t_{33}^+(\lambda) - t_{23}^+(\lambda)t_{32}^+(\lambda)\right),$$

where $t_1^+(\lambda)$ is an analytic transmission function corresponding to $\mathcal{D}_{\rm f}(\lambda)$ and $t_{ij}^+(\lambda)\,, i=2,3$ are four slow-fast transmission functions corresponding to $\mathcal{D}_{\rm s}(\lambda)$. A transmission function measures how much information is transferred to ∞ through the potential given by the square of the front for a function which we fix at $-\infty$. See [vHDK08] for more details and note that the term transmission function comes from scattering theory. Also observe that we use a slightly different notation then [vHDK08], instead of t_i, t_{2i}, and $t_{3i}, i=1,\cdots,6$, we use $t_i^\pm, t_{2i}^\pm$, and $t_{3i}^\pm, i=1,\cdots,3$. We first determine the fast transmission function $t_1^+(\lambda)$.

Lemma B.1. (Fast transmission function) *The fast-fast transmission function $t_1^+(\lambda)$ is of the form*

$$t_1^+(\lambda) = \lambda - \varepsilon^2 \hat{\lambda}_{\rm fast}\,, \tag{B.1}$$

where, to leading order,

$$\hat{\lambda}_{\rm fast} = \frac{6}{\sqrt{2}}\left(\frac{\alpha}{\sqrt{c^2\hat{\tau}^2+4}} + \frac{\beta}{D\sqrt{\frac{c^2\hat{\theta}^2}{D^2}+4}}\right).$$

Proof. From §4.1 in [vHDK08], modified for uniformly traveling fronts, we know that the fast transmission function can be obtained by studying

$$\mathcal{L}u = \lambda u - \varepsilon c u_\eta\,,$$

where $\mathcal{L}$ is defined in Lemma A.1. Moreover, from this work it follows that this problem possibly has positive eigenvalues near zero. Therefore, we write

$$\lambda = \varepsilon\lambda^0 + \varepsilon^2\hat{\lambda}\,.$$

Upon using a regular expansion for $u(\eta)$, that is, $u = u^0 + \varepsilon u^1 + \varepsilon^2 u^2 + \mathcal{O}(\varepsilon^3)$, we obtain

$$\begin{aligned}
\mathcal{O}(1): &\quad \mathcal{L}u^0 = 0\,,\\
\mathcal{O}(\varepsilon): &\quad \mathcal{L}u^1 = \lambda^0 u^0 - c u^0_\eta + 6U^0_{\rm tf}U^1_{\rm tf}u^0\,,\\
\mathcal{O}(\varepsilon^2): &\quad \mathcal{L}u^2 = \lambda^0 u^1 + \hat{\lambda}u^0 - c u^1_\eta + 6U^0_{\rm tf}U^2_{\rm tf}u^0 + 6U^0_{\rm tf}U^1_{\rm tf}u^1 + 3(U^1_{\rm tf})^2 u^0\,.
\end{aligned}$$

The leading order equation yields $u^0(\eta) = C\rho(\eta)$, with $C\in\mathbb{R}$ and ρ defined in (A.1). Applying a solvability condition to the $\mathcal{O}(\varepsilon)$-equation yields

$$0 = \lambda^0 C\int \rho^2 d\eta - cC\int \rho\rho_\eta d\eta + 6C\int U^0_{\rm tf}U^1_{\rm tf}\rho^2 d\eta\,.$$

The last two integrals vanish since they are odd, see Lemma A.1, and since the first integral is unequal to zero, this yields $\lambda^0 = 0$, *i.e.* λ is of $\mathcal{O}(\varepsilon^2)$. Thus, the equation for u^1 becomes

$$\mathcal{L}u^1 = -cC\rho_\eta + 6CU^0_{\rm tf}U^1_{\rm tf}\rho\,.$$

By Lemma A.1, we get that $u^1 = \sqrt{2}C(U^1_{\rm tf})_\eta$. Finally, using all this information, the $\mathcal{O}(\varepsilon^2)$-equation reduces to

$$\mathcal{L}u^2 = C\hat{\lambda}\rho - \sqrt{2}cC(U^1_{\rm tf})_{\eta\eta} + 6CU^0_{\rm tf}U^2_{\rm tf}\rho + 6\sqrt{2}CU^0_{\rm tf}U^1_{\rm tf}(U^1_{\rm tf})_\eta + 3C(U^1_{\rm tf})^2\rho\,,$$

and a solvability condition gives

$$0 = \hat{\lambda} \int \rho^2 d\eta - \sqrt{2}c \int (U_{\mathrm{tf}}^1)_{\eta\eta} \rho d\eta + 6 \int U_{\mathrm{tf}}^0 U_{\mathrm{tf}}^2 \rho^2 d\eta + 6\sqrt{2} \int U_{\mathrm{tf}}^0 U_{\mathrm{tf}}^1 (U_{\mathrm{tf}}^1)_\eta d\eta + 3 \int (U_{\mathrm{tf}}^1)^2 \rho^2 d\eta \ .$$

The last four integral terms are equal up to factor $\sqrt{2}$ to the integral condition in Lemma A.1, and since $\int \rho^2 d\eta = \frac{4\sqrt{2}}{3}$, we get

$$\hat{\lambda} = \frac{6}{\sqrt{2}} \left(\frac{\alpha}{\sqrt{c^2\hat{\tau}^2 + 4}} + \frac{\beta}{D\sqrt{\frac{c^2\hat{\theta}^2}{D^2} + 4}} \right) .$$

This completes the proof of Lemma B.1. □

Lemma B.2. *The slow transmission functions $t_{22}^+, t_{23}^+, t_{32}^+, t_{33}^+$ are given by*

$$\begin{aligned} t_{22}^+(\hat{\lambda}) &= 1 - \frac{2\sqrt{2}}{\sqrt{G_v}} C_2 \,, \qquad t_{23}^+(\hat{\lambda}) = -\frac{2\sqrt{2}}{D\sqrt{G_w}} C_2 \,, \\ t_{32}^+(\hat{\lambda}) &= -\frac{2\sqrt{2}}{\sqrt{G_v}} C_3 \,, \qquad t_{33}^+(\hat{\lambda}) = 1 - \frac{2\sqrt{2}}{D\sqrt{G_w}} C_3 \,, \end{aligned} \tag{B.2}$$

with

$$G_v = c^2\hat{\tau}^2 + 4(\hat{\lambda}\hat{\tau} + 1), \quad G_w = c^2 \frac{\hat{\theta}^2}{D^2} + 4(\hat{\lambda}\hat{\theta} + 1) \,,$$

and C_2 and C_3 are two different integration constants for two different slow basis functions $\Phi_{2,3}$.

Proof. The proof of this lemma is very similar to the derivation of the slow transmission functions in [vHDK08], see especially §4.2 and §5.3. Note that it is even less complicated here since we only make one excursion through a fast field and we do not have to introduce the intermediate transmission functions s_{ij}. Therefore, we omit the proof of this lemma and only state that we need the same asymptotic scalings as in §5.3 of [vHDK08], get the same eigenvalues and eigenvectors, and in the end need to match the slow components and their derivatives over their jump through the fast field I_{f}. □

From Lemma B.2, it follows that

$$t_{22}^+ t_{33}^+ - t_{23}^+ t_{32}^+ = 1 - \frac{2\sqrt{2}}{\sqrt{G_v}} C_2 - \frac{2\sqrt{2}}{D\sqrt{G_w}} C_3 \,,$$

and the Evans function thus reads

$$\mathcal{D}(\hat{\lambda}) = d(\hat{\lambda}) \left(t_1^+(\hat{\lambda}) - \frac{2\sqrt{2}}{\sqrt{G_v}} C_2 t_1^+(\hat{\lambda}) - \frac{2\sqrt{2}}{D\sqrt{G_w}} C_3 t_1^+(\hat{\lambda}) \right) , \tag{B.3}$$

where $d(\hat{\lambda})$ is a nonzero function and note that we suppressed the explicit dependence on $\hat{\lambda}$ in $G_{v,w}$. In order to finish the proof of Theorem 3.4, we need to determine the constants C_2 and C_3. Therefore, we look at the higher order corrections of the fast component of the eigenvalue problem

(3.5) in the fast field $I_{\rm f}$. From the proof of Lemma B.2 it followed that we also need to rescale the slow variables

$$(v,w)(\eta) = \varepsilon(\tilde{v},\tilde{w})(\eta)\,.$$

(Note that the proof of this last lemma is actually not in the present work, but can be found in §5.3 of [vHDK08].) With the above rescalings, the fast u-component of (3.5) becomes

$$u_{\eta\eta} + (1-3(U_{\rm tf})^2)u = -\varepsilon c u_\eta + \varepsilon^2(\alpha\tilde{v} + \beta\tilde{w} + \hat{\lambda}u)\,.$$

Using the regular expansions $u(\eta) = u^0(\eta) + \varepsilon u^1(\eta) + \varepsilon^2 u^2(\eta) + \mathcal{O}(\varepsilon^3)$ and $U_{\rm tf}(\eta) = U^0_{\rm tf}(\eta) + \varepsilon U^1_{\rm tf}(\eta) + \varepsilon^2 U^2_{\rm tf}(\eta) + \mathcal{O}(\varepsilon^3)$, we get

$$\begin{aligned}
\mathcal{O}(1): &\quad \mathcal{L}u^0 = 0\,,\\
\mathcal{O}(\varepsilon): &\quad \mathcal{L}u^1 = -c(u^0)_\eta + 6U^0_{\rm tf}U^1_{\rm tf}u^0\,,\\
\mathcal{O}(\varepsilon^2): &\quad \mathcal{L}u^2 = -c(u^1)_\eta + \alpha\tilde{v} + \beta\tilde{w} + \hat{\lambda}u^0 + 6U^0_{\rm tf}U^1_{\rm tf}u^1 + 6U^0_{\rm tf}U^2_{\rm tf}u^0 + 3(U^1_{\rm tf})^2u^0\,,
\end{aligned}$$

where $\mathcal{L}$ is defined in Lemma A.1. The leading order equation yields that

$$u^0(\eta) = C_{2,3}\rho(\eta),$$

see (A.1), where we use two different constants for the two different slow basis functions $\Phi_{2,3}$. Comparing the $\mathcal{O}(\varepsilon)$-equation with Lemma A.1, yields

$$u^1(\eta) = \sqrt{2}C_{2,3}(U^1_{\rm tf}(\eta))_\eta\,.$$

Finally, integrating the $\mathcal{O}(\varepsilon^2)$-equation against $\rho(\eta)$, and implementing the above expressions for $u^0(\eta)$ and $u^1(\eta)$ gives

$$\begin{aligned}
0 =& -\sqrt{2}cC_{2,3}\int (U^1_{\rm tf})_{\eta\eta}\rho d\eta + \alpha\tilde{v}\int\rho d\eta + \beta\tilde{w}\int\rho d\eta + \hat{\lambda}C_{2,3}\int\rho^2 d\eta\\
&+ 6\sqrt{2}C_{2,3}\int U^0_{\rm tf}U^1_{\rm tf}(U^1_{\rm tf})_\eta\rho d\eta + 6C_{2,3}\int U^0_{\rm tf}U^2_{\rm tf}\rho^2 d\eta + 3C_{2,3}\int (U^1_{\rm tf})^2u^0\rho^2 d\eta\\
=& 2\sqrt{2}\alpha\tilde{v} + 2\sqrt{2}\beta\tilde{w} + 4\frac{\sqrt{2}}{3}\hat{\lambda}C_{2,3} - 8C_{2,3}\left(\frac{\alpha}{\sqrt{c^2\hat{\tau}^2+4}} + \frac{\beta}{D\sqrt{\frac{c^2\hat{\theta}^2}{D^2}+4}}\right)\,,
\end{aligned}$$

where we used the integral condition of Lemma A.1 in the last step and exploited that $\tilde{v}$ and $\tilde{w}$ are the constant values of the slow components in the fast field. When we closely examine the above equation, we recognize the fast transmission function $t_1^+(\hat{\lambda})$ given by (B.1). More precisely, the above equality reduces to

$$0 = \sqrt{2}\alpha\tilde{v} + \sqrt{2}\beta\tilde{w} + C_{2,3}\frac{2\sqrt{2}}{3}t_1^+(\hat{\lambda})\,.$$

Now, we have constructed our slow basis functions in such a fashion that $\tilde{v}=1$ and $\tilde{w}=0$ for Φ_2 and *vice versa* for Φ_3. Therefore, C_2 and C_3 are given by

$$C_2 = -\frac{3}{2}\frac{\alpha}{t_1^+(\hat{\lambda})}\,,\qquad C_3 = -\frac{3}{2}\frac{\beta}{t_1^+(\hat{\lambda})}\,.$$

Implementing this in the Evans function representation of (B.3) gives

$$\begin{aligned}\mathcal{D}(\hat{\lambda}) =& d(\hat{\lambda})\left(t_1^+(\hat{\lambda}) + \frac{3\sqrt{2}}{\sqrt{G_v}}\alpha + \frac{3\sqrt{2}}{\sqrt{G_w}}\frac{\beta}{D}\right)\\ =& d(\hat{\lambda})\left(\hat{\lambda} + 3\sqrt{2}\alpha\left(\frac{1}{\sqrt{c^2\hat{\tau}^2 + 4(\hat{\lambda}\hat{\tau}+1)}} - \frac{1}{\sqrt{c^2\hat{\tau}^2+4}}\right)\right.\\ &\left. +3\sqrt{2}\frac{\beta}{D}\left(\frac{1}{\sqrt{c^2\frac{\hat{\theta}^2}{D^2} + 4(\hat{\lambda}\hat{\theta}+1)}} - \frac{1}{\sqrt{\frac{c^2\hat{\theta}^2}{D^2}+4}}\right)\right),\end{aligned}$$

which completes the proof of Theorem 3.4.

C Number of small eigenvalues (Proof of Lemma 3.6)

We examine the roots of the Evans function (3.6), that is, of

$$E(\hat{\lambda}) = \hat{\lambda} + 3\sqrt{2}\left(F_0 + F(\hat{\lambda})\right),$$

where $F(\hat{\lambda}) = \alpha\sqrt{F_1} + \frac{\beta}{D}\sqrt{F_2}$ and

$$F_0 = -\frac{\alpha}{\sqrt{c^2\hat{\tau}^2+4}} - \frac{\beta}{\sqrt{c^2\hat{\theta}^2+4D^2}}, \quad F_1(\hat{\lambda}) = \frac{1}{c^2\hat{\tau}^2+4+4\hat{\tau}\hat{\lambda}}, \quad F_2(\hat{\lambda}) = \frac{1}{c^2\hat{\theta}^2/D^2+4+4\hat{\theta}\hat{\lambda}}.$$

We shall prove in this section that E possesses at most three (complex) roots. Since one of these is always zero, in case of two roots the other one must be real, and if there are three, either all are real or the nonzero ones form a complex conjugate pair. In fact, we shall prove that for $\alpha, \beta > 0$ there are precisely two real eigenvalues, for $\alpha, \beta \leq 0$ there is one, and in case $\alpha\beta < 0$ we give conditions for when the number is one or three.

Let us briefly relate this to the spectrum of the linearization $\mathbb{L}_c$ in a front, where changes in the number of roots of E are changes in the number of eigenvalues. In the analysis below, we find that eigenvalues are lost to or born from a branch cut $B_* \subset \mathbb{R} - \backslash\{0\}$ for E. This relates to the spectral theory of $\mathbb{L}_c$ via the so-called absolute spectrum as defined in [SS00], which is the branch cut in our case and more generally the boundary for analytic continuations of an Evans function [SS04].

Before entering into the proof, we make some preliminary observations on the domain and holomorphic (analytic) nature of E. Clearly, $E(\hat{\lambda}) = \hat{\lambda}$ for $\alpha = \beta = 0$, which is holomorphic on $\mathbb{C}$ and has zero as its only root. Concerning singularities and the occurrence of square root terms $\sqrt{F_j}$ in E, these can cancel each other in the sense that $F \equiv 0$ for $\alpha\beta \neq 0$ if and only if $\alpha\beta < 0$ and the two square root terms merge into a single one. The latter means that the possible singularities in $\hat{\lambda}$, given by

$$\hat{\lambda}_{\hat{\tau}} = -\frac{1}{\hat{\tau} - \frac{c^2\hat{\tau}}{4}}, \qquad \hat{\lambda}_{\hat{\theta}} = -\frac{1}{\hat{\theta} - \frac{c^2\hat{\theta}}{4D^2}}$$

are equal, which is equivalent to

$$\frac{c^2}{4}\left(\hat{\tau}-\frac{\hat{\theta}}{D^2}\right)+\frac{1}{\hat{\tau}}-\frac{1}{\hat{\theta}}=0. \tag{C.1}$$

If in addition $\Sigma = 0$, where

$$\Sigma := \frac{\alpha}{\sqrt{\hat{\tau}}}+\frac{\beta}{D\sqrt{\hat{\theta}}}, \tag{C.2}$$

then both $F(\lambda)$ and F_0 vanish. In case (C.1) and (C.2) hold we have $E(\hat{\lambda}) = \hat{\lambda}$, as for $\alpha = \beta = 0$. Simple examples for (C.1) are $\hat{\tau} = \hat{\theta}$, and $c = 0$ or $D = 1$. (Recall that we have stipulated that $D > 1$. However, this is not necessary for this proof.) If, in addition, $\alpha = -\beta/D$ then also (C.2) is fulfilled.
Notably, condition (C.1) is independent of α, β, which is a splitting of parameter space we shall exploit later.

In the generic case, where (C.2) fails, the nature of E is different. We understand square roots as the principal branch with branch cut the negative real axis, that is, $\hat{\lambda} \in \mathbb{C}$ has arguments in $(-\pi, \pi]$, and the image of the square roots has non-negative real parts. Hence, the images of $\sqrt{F_j}$ have non-negative real parts and E is holomorphic only on $\mathbb{C} \setminus B_*$ with branch cut for E being the half line $B_* := (-\infty, \max(\hat{\lambda}_{\hat{\tau}}, \hat{\lambda}_{\hat{\theta}})] \subset \mathbb{R}_- \setminus \{0\}$, where $\hat{\lambda}_{\hat{\tau}}$ and $\hat{\lambda}_{\hat{\theta}}$ defined above are the branch points and also singularities of E.

The proof that there are at most three roots goes by a homotopy argument to a case of merged singularities (C.1). Before entering into the homotopy, we proceed with following preliminary observations, where the number of roots is understood to be counted with multiplicity.

Lemma C.1. *Assume $(\alpha, \beta) \neq (0, 0)$ and $D, \hat{\tau}, \hat{\theta} > 0$.*

(i) *For $\alpha\beta \neq 0$ there are no roots of E in the closed interval between the singularities $\hat{\lambda}_{\hat{\tau}}$ and $\hat{\lambda}_{\hat{\theta}}$.*

(ii) *Suppose $\alpha = 0$ or $\beta = 0$, or (C.1) holds, and define Σ as in (C.2). Then E has precisely two roots if $\Sigma > 0$ and one, if $\Sigma \leq 0$. None of these roots lies in B_*.*

(iii) *For $\alpha\beta \neq 0$, E possesses a root $\hat{\lambda}_B \in B := (-\infty, \min(\hat{\lambda}_{\hat{\tau}}, \hat{\lambda}_{\hat{\theta}})] \subset B_*$ if and only if $\alpha\beta < 0$, $\hat{\lambda}_B = \frac{3\sqrt{2}\alpha}{\sqrt{c^2\hat{\tau}^2+4}} + \frac{3\sqrt{2}\beta}{\sqrt{c^2\hat{\theta}^2+4D^2}} \in B$, and α, β lie on the curves of the hyperbolic conic section $\mathcal{C}$ in the (α, β)-plane given by $A\alpha^2 + a\alpha = B\beta^2 + b\beta$ with strictly positive*

$$A = \frac{3\sqrt{2}}{\hat{\tau}},\ B = A\frac{\hat{\tau}}{D^2\hat{\theta}},\ a = \sqrt{c^2\hat{\tau}^2+4}\frac{c^2\hat{\theta}^2+4D^2}{4\hat{\tau}\hat{\theta}D^2},\ b = \sqrt{c^2\hat{\theta}^2+4D^2}\frac{c^2\hat{\tau}^2+4}{4\hat{\tau}\hat{\theta}D^2}.$$

Such a root of E is simple (on the principal part of the square roots).

(iv) *If $E(\lambda) = 0$ then $p(z) = 0$, where $z = \sqrt{c^2\hat{\tau}^2 + 4(\hat{\tau}\lambda + 1)}$ and $p(z)$ is a polynomial of degree at most 8 with real coefficients. In particular, E has at most 8 roots and for any bounded parameter set there is an $R > 0$ such that there is no root of E with modulus larger than or equal to R for parameters chosen from this set.*

Proof. **(i)** For $\hat{\lambda}$ between the singularities, exactly one of the square root terms involving $\hat{\lambda}$ is purely imaginary while all other terms are real. Hence, the imaginary part of E is given by the reciprocal of a square root, and as such never vanishes on its domain.

(ii) In all cases only one square root term in E involving $\hat{\lambda}$ remains, and $E = 0$ can be arranged to read $\hat{\lambda} - \Sigma C_1/\sqrt{C_2} = -\Sigma C_1/\sqrt{C_2 + \hat{\lambda}}$, where $C_1, C_2 > 0$. Upon rescaling $\tilde{\lambda} = \hat{\lambda}/C_2$ and setting $C = C_1/C_2^{3/2}$ this becomes

$$\tilde{\lambda} - \Sigma C = -\Sigma C/\sqrt{1 + \tilde{\lambda}}. \tag{C.3}$$

Let us consider $\tilde{\lambda} \in \mathbb{R}$ first and note that $C > 0$. Then the left hand side of (C.3) is always real, but the right hand side is not for $\tilde{\lambda} < -1$, that is, $\hat{\lambda}$ is in the interior of B. Hence, there are no roots on B. For $\tilde{\lambda} \geq -1$, the graph of the left hand side of (C.3) is always a line with positive slope, which meets the graph of the right hand side at $\tilde{\lambda} = 0$. The latter is concave and unbounded for $\Sigma > 0$, which generates two intersections counted with multiplicity. In case $\Sigma \leq 0$ the only intersection point is $\tilde{\lambda} = 0$.

Upon squaring both sides in the above equation and multiplying by the denominator, we find a polynomial of degree three, which means there are at most three complex roots. Dividing by $\tilde{\lambda}$ this polynomial reduces to

$$\tilde{\lambda}^2 + (1 - 2\Sigma C)\tilde{\lambda} + (\Sigma C - 2)\Sigma C = 0.$$

Since roots come in complex conjugate pairs, the fact that for $\Sigma > 0$ there are two real roots already proves that a third non-real solution is not possible and so there are precisely two real ones. In the case $\Sigma < 0$ we can rule out a complex conjugate pair of roots as follows. From the quadratic equation we infer that the real part of such roots would be $\Sigma C - 1/2 < 0$ so that the left hand side of (C.3) in this root has negative real part. However, the right hand side has positive coefficient in this case and the principal branch of the square root has non-negative real parts. Hence, also the reciprocal has positive real part and so for $\Sigma < 0$ the only root is $\hat{\lambda} = 0$.

(iii) For $\hat{\lambda} \in B$ both square root terms in E involving $\hat{\lambda}$ are purely imaginary, and the real part of E reads

$$\hat{\lambda} - \frac{3\sqrt{2}\alpha}{\sqrt{c^2\hat{\tau}^2 + 4}} - \frac{3\sqrt{2}\beta}{\sqrt{c^2\hat{\theta}^2 + 4D^2}},$$

which gives the claimed location of $\hat{\lambda}$, and since $\mathrm{Re}(\partial_{\hat{\lambda}} E(\hat{\lambda}_B)) = 1$ it is a simple root. As the imaginary part is a sum of square root reciprocals, it can only vanish if these have opposing sign, which means $\alpha\beta < 0$. Substituting the location of $\hat{\lambda}$ and dividing out the trivial root $\hat{\lambda} = 0$, a straightforward calculation yields the claimed conic section.

(iv) Set $z^2 = c^2\hat{\tau}^2 + 4(\hat{\tau}\hat{\lambda} + 1)$, that is, $\hat{\lambda} = (z^2 - c^2\hat{\tau}^2 - 4)/(4\hat{\tau})$ and substitute this into $E(\hat{\lambda})$. Then, using $z = \sqrt{z^2}$, at most one square root term involving z^2 remains and $E = 0$ can be arranged so that the right hand side is a pure square root. Upon squaring, the left hand side is the sum of a rational function with numerator of degree at most 4 and denominator of degree at most 2. The right hand side is the reciprocal of an at most quadratic polynomial so that the equation can be rearranged as $p(z) = 0$ with suitable polynomial p of degree at most

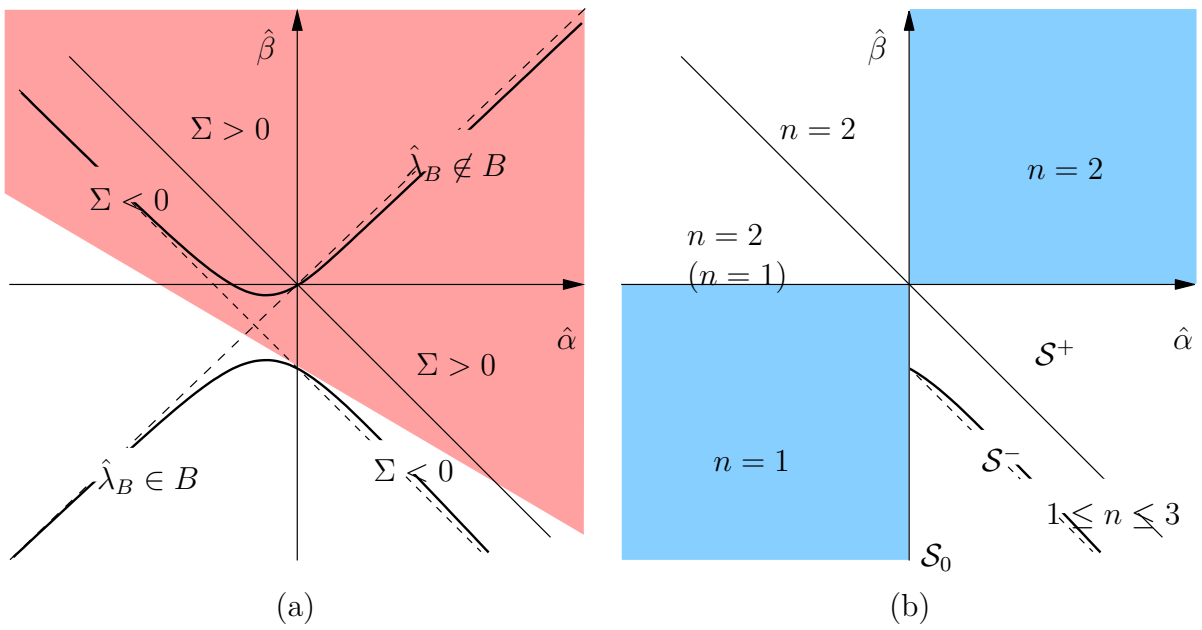

FIGURE 12: Schematic illustrations in case $\hat\lambda_{\hat\tau} > \hat\lambda_{\hat\theta}$. (a) the conic section, $\mathcal{C}$, at the beginning of the homotopy (bold) and at the end (dashed), and the region where $\hat\lambda_B \notin B$ (shaded), as well as the signs of Σ in the various regions. (b) The relevant part of $\mathcal{C}$, $\mathcal{C}^*$, at the beginning of the homotopy to (C.1) (bold) and at the end (dashed). The numbers of roots, n, in the various regions inside the homotopy. The shaded regions have $\alpha\beta > 0$.

8 with real coefficients. Compare (C.5) below. Its at most 8 complex roots are confined to a bounded region and continuous dependence of roots on the parameters gives R.

□

We are now ready to prove Lemma 3.6. Figure 12 illustrates the setting.

For parameters as in item **(ii)** of Lemma C.1, the claim holds so that we next assume parameters with $\alpha\beta \neq 0$ and where (C.1) fails, i.e., $\hat\lambda_{\hat\tau} \neq \hat\lambda_{\hat\theta}$.

The case $\alpha\beta > 0$. For $\alpha\beta > 0$, take any homotopy in $(c, D, \hat\tau, \hat\theta)$ from the given parameters to a point for which (C.1) holds, for instance to $D = 1, \hat\tau = \hat\theta$. Clearly, during the homotopy there is no sign change of α and β. Lemma C.1, **(iv)**, provides an R so that there is no root on $\{|z| = R\}$ during the homotopy and Lemma C.1, **(i)**, **(iii)** for $\alpha\beta > 0$, imply that there are no roots on the branch cut B_* during this homotopy. Since $\alpha\beta > 0$ we readily estimate that the (finitely many) roots stay uniformly away from the singularities and hence from B_*. This provides an open neighborhood U of B_* without roots during the homotopy. Now E is holomorphic in the closed simply connected set $G = \{z \in \mathbb{C} : |z| \leq R\} \setminus U$ and there are no roots on ∂G during the homotopy. Hence, the number of roots of E in G remains constant during the entire homotopy. Therefore, Lemma C.1, **(ii)**, implies that E possesses up to two roots in $\mathbb{C} \setminus U$ also for the initially given parameters, and since there are none in U this also holds in $\mathbb{C}$. More precisely, $\alpha, \beta > 0$ implies $\Sigma > 0$ so that by Lemma C.1, **(ii)**, there are two roots, and $\alpha, \beta < 0$ implies $\Sigma < 0$ so that there is one root in this case.

The case $\alpha\beta < 0$. If we still can choose a homotopy to a point where (C.1) holds such that no root approaches B during the homotopy, the argument for $\alpha\beta > 0$ applies and it follows that there are one or two roots depending on the sign of Σ. However, this is not possible in general. The two main points to consider are the possible gain or loss of roots when crossing $\mathcal{C}$ and at the endpoint of the homotopy. Let n denote the parameter dependent number of roots. The strategy in the following to show that a homotopy in $(c, D, \hat{\tau}, \hat{\theta}, \alpha, \beta)$ can be chosen so that

(a) n changes at most by two when crossing $\mathcal{C}$,

(b) at most one (and usually no) such crossing occurs during the homotopy,

(c) at the homotopy endpoint, n changes in such a way that $1 \leq n \leq 3$ throughout the homotopy. In fact, the precise number of roots in different regions in parameter space will be derived.

(a) Crossing $\mathcal{C}$. Assume parameters lie on $\mathcal{C}$ so that there exists a simple and unique root $\lambda_B \in B$ according to Lemma C.1 **(iii)**. To see all Riemann surface branches, consider the multivalued images of the square root terms and record all λ on the principal branch with argument in $(-\pi, \pi]$ upon perturbing parameters. The four sign distributions on the square roots in F yield all images $E^s_\sigma(\lambda) = \lambda + F_0 + \sigma\sqrt{F_1(\lambda)} + s\sqrt{F_2(\lambda)}$, $\sigma, s \in \{-1, +1\}$, where we drop the 1's to ease notation so that $E = E^+_+$ is the image on the principal branch. For $\lambda \in B$ the square root term images in F form two complex conjugate pairs on the imaginary axis, while $\hat{\lambda} + F_0$ is real. Thus, $\mathrm{Im}(E^+_+(\lambda_B)) = 0$ implies $F(\lambda_B) = 0$ and hence $E^-_-(\lambda_B) = 0$, while $E^+_-(\lambda), E^-_+(\lambda) \neq 0$ since (C.1) fails. The analytic continuation of E^s_σ yields continuous curves of roots (and typically a branch switching), so that the only possible roots on the principal branch for perturbations of parameters away from $\mathcal{C}$ are continuations of λ as roots of the analytic continuations of E^+_+ or E^-_-. But this means that typically n changes by two if the root crosses B as parameters cross $\mathcal{C}$. Indeed, this always occurs as implicit differentiation shows: let us write E in the compact form

$$E(\hat{\lambda}) = \hat{\lambda} + F_0 + \frac{c_1}{\sqrt{c_2 + \hat{\lambda}}} + \frac{c_3}{\sqrt{c_4 + \hat{\lambda}}}, \tag{C.4}$$

with $c_1 = \beta/(2D\sqrt{\theta})$, $c_2 = -\hat{\lambda}_{\hat{\theta}}$, $c_3 = \alpha/(2\sqrt{\hat{\tau}})$, $c_4 = -\hat{\lambda}_{\hat{\tau}}$. Since $\hat{\lambda}_B$ is a simple root the implicit function theorem applies to its parameter dependence. Since $c_1 \neq 0$ ($\alpha\beta < 0$) let us consider the c_1-dependence of this root; dependencies on other parameters driving off $\mathcal{C}$ are analogous. From

$$\mathrm{Im}(\partial_{c_1} E(\hat{\lambda}_B)) = \frac{1}{\sqrt{-c_2 - \hat{\lambda}_B}} \neq 0$$

it follows that roots cross the branch cut B when parameters cross $\mathcal{C}$, and hence move to another branch of the Riemann surface, and n changes by two.

In particular, when the initial parameters lie on $\mathcal{C}$ and $\hat{\lambda}_B \in B$, the number of roots lies between the numbers of roots near $\mathcal{C}$.

(b) Number of crossings of $\mathcal{C}$. In order to choose a homotopy that avoids unnecessary crossings of $\mathcal{C}$, we normalize $\mathcal{C}$ by rescaling $\hat{\beta} = \frac{b}{B}\beta$, and then $\hat{\alpha} = \frac{b}{\sqrt{AB}}\alpha$, which changes $\mathcal{C}$ to $\hat{\mathcal{C}}$ given by

$\hat\alpha^2 + \hat a\hat\alpha = \hat\beta^2 + \hat\beta$ with

$$\hat a = \frac{a}{b}\sqrt{\frac{B}{A}} = \sqrt{\frac{c^2\hat\theta^2 + 4D^2}{c^2\hat\tau + 4}\frac{\hat\tau}{D^2\hat\theta}} = \sqrt{\frac{c^2/D^2 + 4/\hat\theta}{c^2 + 4/\hat\tau}} = \sqrt{\frac{\hat\lambda_{\hat\theta}}{\hat\lambda_{\hat\tau}}}.$$

Note that a homotopy to a point that satisfies (C.1), i.e., $\hat\lambda_{\hat\theta} = \hat\lambda_{\hat\tau}$, is a homotopy of $\hat a$ to 1. The formula for $\hat a$ yields a homotopy so that $\hat a$ monotonically grows or decays to 1, e.g., changing $\hat\tau$ only. This homotopy yields a homotopy in $\{\alpha\beta \neq 0\}$ such that $(\hat\alpha, \hat\beta)$ remain unchanged during the homotopy that changes $\hat a$. Since a fixed $(\hat\alpha, \hat\beta)$ lies on $\hat{\mathcal{C}}$ at a unique value of $\hat a$, it follows that there is at most one crossing of $\hat{\mathcal{C}}$ during the combined homotopy, which will be the homotopy in the following.

In fact, only the branch of $\mathcal{C}$ contained in $\{\Sigma < 0\}$ is relevant at all, and there is no crossing for $\Sigma > 0$ as shown next.

The relevant component of $\mathcal{C}$: $\mathcal{C}^*$. Let us check the condition $\hat\lambda_B \in B$, that is, $\hat\lambda_B < \min\{\hat\lambda_{\hat\tau}, \hat\lambda_{\hat\theta}\}$ from Lemma C.1 **(iii)** on $\mathcal{C}$. Substituting the formulas for these quantities, we readily compute that the $(\hat\alpha, \hat\beta)$-value for $\hat\lambda_B = \min\{\hat\lambda_{\hat\tau}, \hat\lambda_{\hat\theta}\}$ lies on one branch of $\mathcal{C}$. More precisely, for $\hat\lambda_{\hat\tau} < \hat\lambda_{\hat\theta}$ this point lies at $\hat\alpha = 0$, $\hat\beta = -1$ and for $\hat\lambda_{\hat\tau} > \hat\lambda_{\hat\theta}$ at $\hat\alpha = -\hat a$, $\hat\beta = 0$. Since $\hat\lambda_B$ cannot cross a singularity as $(\hat\alpha, \hat\beta)$ move on a curve of $\mathcal{C}$, the line $\{\hat\lambda_B = \hat\lambda_{\hat\tau}\}$ is tangent to $\mathcal{C}$ at the intersection point; compare Figure 12(a). Due to the conic section geometry, the line does not cross the other branch of $\mathcal{C}$. Since increasing $\hat\alpha$ means increasing $\hat\lambda_B$, the other branch of $\mathcal{C}$ has $\hat\lambda_B \notin B$. Therefore, always only the branch of $\mathcal{C}$ in the region $\{\Sigma < 0\}$ is relevant; denote this by $\mathcal{C}^*$.

The location of $\mathcal{C}^*$, $\operatorname{sgn}(\Sigma)$ and the set $\pm_0$. To show $\mathcal{C}^*$ is contained in $\{\Sigma < 0\}$, consider the sign of Σ during the homotopy. It follows from (C.2) that

$$\operatorname{sgn}(\Sigma) = \operatorname{sgn}\left(\sqrt{A}\alpha + \sqrt{B}\beta\right) = \operatorname{sgn}(\hat\Sigma),\ \hat\Sigma := \hat\alpha + \hat\beta.$$

Together with the fact that $\hat{\mathcal{C}}$ can be written as

$$\hat\alpha = -\frac{\hat a}{2} \pm \sqrt{\frac{\hat a^2}{4} + \hat\beta^2 + \hat\beta},$$

we readily infer that $\Sigma = 0$, i.e., $\hat\alpha = -\hat\beta$, requires $\hat a = -1$, which is outside the homotopy range. Therefore, $\{\Sigma = 0\}$ is disjoint from $\mathcal{C}$ during the homotopy (recall that $\mathcal{C}$ and also $\hat{\mathcal{C}}$ change during the homotopy). Hence, since either $(\hat\alpha, \hat\beta) = (-\hat a, 0)$ or $(0, -1)$ lies on $\hat{\mathcal{C}}^*$ and has $\Sigma < 0$, it holds that $\Sigma < 0$ on the entire $\mathcal{C}^*$ in $\{\hat\alpha\hat\beta < 0\}$ and during the homotopy. In conclusion, crossing $\hat{\mathcal{C}}^*$ in case $\alpha\beta < 0$ requires $\Sigma < 0$. Moreover, since the homotopy makes a locally bounded monotone change in $\hat{\mathcal{C}}$, there is an open region within $\{\hat\Sigma < 0\}$ that is disjoint from all $\hat{\mathcal{C}}$ during the homotopy. Let $\pm_0$ denote this set; compare Figure 12(b).

(c) Change of n at the homotopy endpoint. Next to crossing $\mathcal{C}^*$, the only possible change in the number of roots are bifurcations from the branch point at the end of the homotopy. (Due to Lemma C.1, this cannot happen in the interior of B_*, and roots remain away from the disjoint singularities inside the homotopy.) Recall that the singularities, $\hat\lambda_{\hat\tau}, \hat\lambda_{\hat\theta}$, merge into the branch point

at the end of the homotopy, where (C.1) holds. Consider the form (C.4) of E with $c_4 = c_2 + \delta \geq c_2$ so that in case $\hat{\lambda}_{\hat{\tau}} < \hat{\lambda}_{\hat{\theta}}$ we have $c_1 = \beta/(2D\sqrt{\theta})$, $c_3 = \alpha/(2\sqrt{\hat{\tau}})$ and $c_2 = \hat{\lambda}_{\hat{\theta}}$, $\delta = \hat{\lambda}_{\hat{\theta}} - \hat{\lambda}_{\hat{\tau}}$. Otherwise c_1 and c_3 are interchanged and $c_2 = \hat{\lambda}_{\hat{\theta}}$. Note that always $c_1 + c_3 = \Sigma$. Since we are concerned only with roots approaching $-c_2$, we write $\hat{\lambda} = w^2 - c_2$, $w \in \mathbb{C}$, which gives

$$F(w^2 - c_2) = \left(\frac{c_1}{w} + \frac{c_3}{\sqrt{w^2 + \delta}} \right).$$

The full Evans function in this form, denoted by E_δ, reads $E_\delta(w^2) = w^2 - c_2 + F_0 + F$ and roots satisfy

$$w^2 - c_2 + F_0 + \frac{c_1}{w} = -\frac{c_3}{\sqrt{w^2 + \delta}}.$$

Upon squaring and multiplication by denominators this yields the polynomial equation

$$P_\delta(w) := (w^3 + (F_0 - c_2)w + c_1)^2(w^2 + \delta) - c_3^2 w^2 = 0. \tag{C.5}$$

We readily compute that $P_0(0) = 0$, $\partial_w P_0(0) = 0$, and $\partial_w^2 P_0(0) = 2(c_1^2 - c_3^2)$. Hence, in $\{\alpha\beta < 0\}$ we have $\partial_w^2 P_0(0) = 0$ if and only if $\Sigma = 0$, which means that in $\{\alpha\beta < 0, \Sigma \neq 0\}$ precisely two roots of P_δ bifurcate from $w = 0$ at $\delta = 0$. (Here we suppressed the dependence of c_j on δ, which is irrelevant for the argument.)

However, these bifurcating roots are not necessarily roots of E_δ. Indeed, consider the bifurcation of real roots, which, away from $\mathcal{C}^*$, is necessarily for $z = w^2 > 0$. Here the graph of E_δ converges locally uniformly to that of E_0 as $\delta \to 0$. See Figure 13(a). We readily check that $\partial_z^2 E_\delta$ has a unique positive root for $\delta > 0$, so that the only option for a change in the number of roots is a change by one through a sign change of the asymptotics as $z \to 0$. If $\delta > 0$ we have $\operatorname{sgn}(F) = \operatorname{sgn}(c_1)$, while $\operatorname{sgn}(F) = \operatorname{sgn}(c_1 + c_3)$ for $\delta = 0$. Hence, if $\operatorname{sgn}(c_1) = \operatorname{sgn}(c_1 + c_3)$ no real roots bifurcate, while for $\operatorname{sgn}(c_1) \neq \operatorname{sgn}(c_1 + c_3)$ one real root is lost as $\delta \to 0$.

Which case occurs in terms of the original parameters depends on the ordering of singularities. For $\hat{\lambda}_{\hat{\tau}} < \hat{\lambda}_{\hat{\theta}}$ ($\hat{\lambda}_{\hat{\tau}} > \hat{\lambda}_{\hat{\theta}}$) a change of n by one occurs when $\operatorname{sgn}(\alpha) \neq \operatorname{sgn}(\Sigma)$ ($\operatorname{sgn}(\beta) \neq \operatorname{sgn}(\Sigma)$) and otherwise n remains constant or changes by two. Therefore, n can change by two at the end of the homotopy only in the component of $\{\alpha\beta < 0, \Sigma \neq 0\}$ that contains $\mathcal{C}^*$. Compare Figure 12(b).

Counting roots. Let us now gather what we learned about the number of roots n: in the quadrant of $\{\alpha\beta < 0\}$ containing the irrelevant branch of the conic section, $\mathcal{C} \setminus \mathcal{C}^*$, n can only change at the end of the homotopy, where $n = 2$ for $\Sigma > 0$ and $n = 1$ for $\Sigma < 0$. Since such a change is at most by one, it follows that inside the homotopy (i.e. without the endpoint) $n = 2$ in this quadrant of $\{\alpha\beta < 0\}$.

Within the quadrant of $\{\alpha\beta < 0\}$ containing $\mathcal{C}^*$, let $\pm^-$ denote the subset where $\Sigma < 0$ and $\pm^+$ where $\Sigma > 0$. In $\pm^+$, n changes at the end of the homotopy, where it drops by one, so that inside the homotopy $n = 3$, and this extends to $\{\Sigma = 0\}$. In $\pm^-$ we have $n = 1$ at the end of the homotopy from a possible drop by one or two, so that $1 \leq n \leq 3$ inside the homotopy.

In conclusion, $1 \leq n \leq 3$ for all parameter values. More precisely, the global distribution of n in parameter space is as follows; see Figure 13(b): n must be constant (inside the homotopy) in the

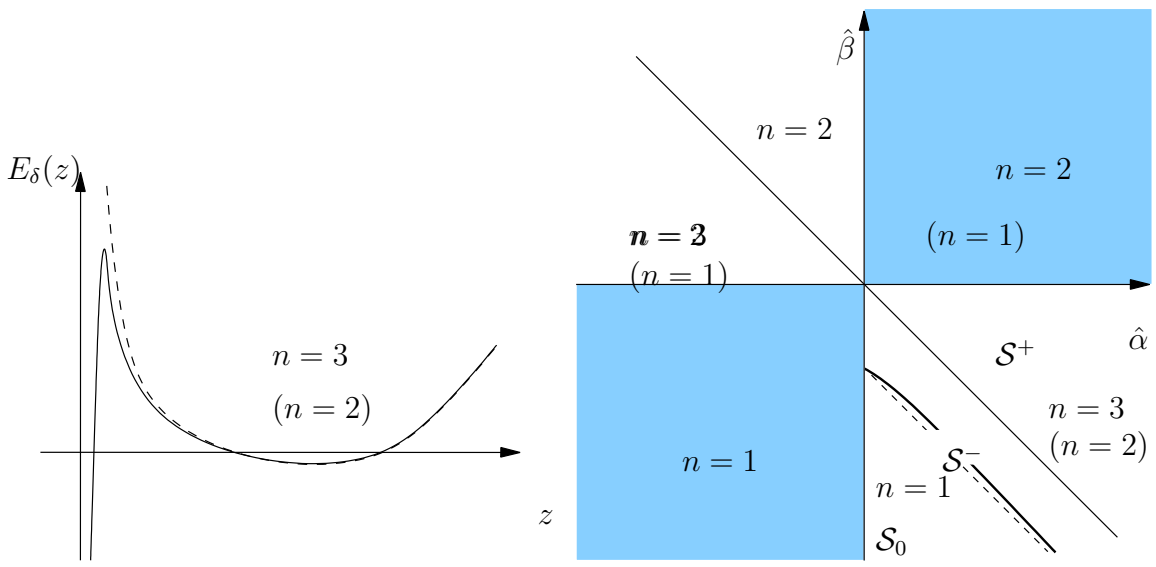

(a) (b)

-45

FIGURE 13: In both panels n in brackets is the value at the end of the homotopy, if different from inside the homotopy in the given region. (a) Sketch of the graphs of E_δ for $\delta > 0$ (solid) and $\delta = 0$ (dashed) illustrating the loss of one real root into the branch point $z = 0$, which occurs for $\operatorname{sgn}(\beta) \neq \operatorname{sgn}(\Sigma)$ if $\hat\lambda_{\hat\tau} > \hat\lambda_{\hat\theta}$, and for $\operatorname{sgn}(\alpha) \neq \operatorname{sgn}(\Sigma)$ if $\hat\lambda_{\hat\tau} < \hat\lambda_{\hat\theta}$. (b) The distribution of n in case $\hat\lambda_{\hat\tau} > \hat\lambda_{\hat\theta}$ with curves and regions are as in Figure 12(b).

connected components of $\{\hat\alpha\hat\beta < 0\} \setminus \mathcal{C}^*$. Since crossing $\{\Sigma = 0\}$ does not change the number of roots we have $n = 3$ in the component containing $\pm^+$. Since crossing $\mathcal{C}^*$ changes n by two it follows that $n = 1$ in the component containing $\mathcal{S}_0$.

References

[AGJ90] J. Alexander, R.A. Gardner, C.K.R.T. Jones. A topological invariant arising in the stability analysis of travelling waves. *J. für die Reine und Angewandte Mathematik*, 410, 167–212 (1990).

[BDKP13] T. Bellsky, A. Doelman, T.J. Kaper, K. Promislow Adiabatic stability under semi-strong interactions: the weakly damped regime. *To appear in Indiana Univ. Math. J.*, (2013).

[CW09] W. Chen, M.J. Ward. Oscillatory instabilities of multi-spike patterns for the one-dimensional Gray-Scott model. *European J. Appl. Math.*, 20, no. 2, 187–214 (2009).

[CC12] Ch.-N. Chen, Y.S. Choi. *Arch. Rat. Mech. Anal.*, 206, no. 3, 741–777 (2012).

[CP89] J. Carr, R. Pego. Metastable patterns in solutions of $u_t = \varepsilon^2 u_{xx} - f(u)$ *Comm. Pure Appl. Math.*, 42, Issue 5, 523-576 (1989).

[DEK01] A. Doelman, W. Eckhaus, T. J. Kaper. Slowly modulated two-pulse solutions in the Gray–Scott model II: Geometric theory, bifurcations, and splitting dynamics. *SIAM J. Appl. Math.*, 61, no. 6, 2036–2062 (2001).

[DGK98] A. Doelman, R.A. Gardner, T.J. Kaper. Stability analysis of singular patterns in the 1-D Gray–Scott model: a matched asymptotics approach. *Physica D*, 122, no. 1–4, 1–36 (1998).

[DGK01] A. Doelman, R.A. Gardner, T.J. Kaper. Large stable pulse solutions in reaction-diffusion equations. *Indiana Univ. Math. J.*, 50, no. 1, 443–507 (2001).

[DGK02] A. Doelman, R.A. Gardner, T.J. Kaper. A stability index analysis of 1-D patterns of the Gray-Scott model. *Mem. Amer. Math. Soc.*, 155, no. 737 (2002).

[DvHK09] A. Doelman, P. van Heijster, T.J. Kaper. Pulse dynamics in a three-component system: existence analysis. *J. Dyn. Diff. Eq.*, 21, 73–115 (2009).

[DK03] A. Doelman, T.J. Kaper. Semistrong pulse interactions in a class of coupled reaction-diffusion equations. *SIAM J. Applied Dyn. Sys.*, 2, no. 1, 53–96 (2003).

[DKP07] A. Doelman, T.J. Kaper, K. Promislow Nonlinear asymptotic stability of the semistrong pulse dynamics in a regularized Gierer-Meinhardt model. *SIAM J. Math. Anal.*, 38, no. 6, 1760–1787 (2007).

[Ei02] S.-I. Ei. The motion of weakly interacting pulses in reaction-diffusion systems. *J. Dyn. Diff. Eq.*, 14, 85–137 (2002).

[EIK08] S.-I. Ei, H. Ikeda, T, Kawana. Dynamics of front solutions in a specific reaction-diffusion system in one dimension. *Japan J. Indust. Appl. Math.*, 25, no. 1, 117–147 (2008).

[EMN02] S.-I Ei, M. Mimura, M. Nagayama. Pulse-pulse interaction in reaction-diffusion systems. *Physica D*, 165, no. 3-4, 176–198 (2002).

[FH89] G. Fusco, J.K. Hale. Slow-motion manifolds, dormant instabilities and Singular Perturbations. *J. Dyn. Diff. Eq.*, 1, 75–94 (1989).

[HI11] M. Haragus, G. Iooss. Local Bifurcations, Center manifolds, and normal forms in infinite-dimensional dynamical systems. *Springer-Verlag London, Ltd., London; EDP Sciences, Les Ulis* (2011).

[vHDK08] P. van Heijster, A. Doelman, T.J. Kaper. Pulse dynamics in a three-component system: stability and bifurcations. *Physica D*, 237, 3335–3368 (2008).

[vHDKP10] P. van Heijster, A. Doelman, T.J. Kaper, K. Promislow. Front interactions in a three-component system. *SIAM J. Applied Dyn. Sys.*, 9, no. 2, 292–332 (2010).

[vHS11] P. van Heijster, B. Sandstede. Planar radial spots in a three-component FitzHugh-Nagumo system. *Journal of Nonlinear Science*, 21, 705–745 (2011).

[Hen81] D. Henry. Geometric theory of semilinear parabolic equations. *Lecture Notes in Mathematics* 840 Springer-Verlag, Berlin-New York, (1981).

[Jo95] C.K.R.T. Jones. Geometric singular perturbation theory. *Lecture Notes in Math.* 1609, Springer, Berlin, Dynamical systems, 44–118 (1995).

[KNO90] H. Kokubu, Y. Nishiura, H. Oka. Heteroclinic and homoclinic bifurcations in bistable reaction diffusion systems. *J. Diff. Eq.*, 86, no. 2, 260–341 (1990).

[KWW06] T. Kolokolnikov, M.J. Ward, J. Wei. Zigzag and breakup instabilities of stripes and rings in the Two-Dimensional Gray-Scott Model. *Stud. in Appl. Math.*, 16, no. 1, 35–95 (2006).

[KWY13] T. Kolokolnikov, J. Wei, W. Yang. On Large ring solutions for Gierer-Meinhardt system in $\mathbb{R}^3$. *J. Diff. Eq.*, 255, no. 7, 1408–1436 (2013).

[NTU03] Y. Nishiura, T. Teramoto, K.-I. Ueda. Scattering and separators in dissipative systems. *Phys. Rev. E* 67, 056210 (2003).

[NTYU07] Y. Nishiura, T. Teramoto, X. Yuan, K.-I. Ueda. Dynamics of traveling pulses in heterogeneous media. *Chaos*, 17, no. 3, 037104 (2007).

[NU01] Y. Nishiura, D. Ueyama. Spatio-temporal chaos for the Gray-Scott model. *Phys. D*, 150, 137–162, (2001).

[Pe93] J. E. Pearson. Complex patterns in a simple system. *Science*, 261, 189–192 (1993).

[PS96] T. Poston, I. Stewart. Catastrophe theory and its applications. *Dover Publications* (1996).

[Pro02] K. Promislow. A renormalization method for modulational stability of quasi-steady patterns in dispersive systems. *SIAM J. Math. Anal.*, 33, no. 6, 1455–1482 (2002).

[Ra13] J.D.M. Rademacher. First and second order semi-strong interaction in reaction-diffusion systems. *SIAM J. Appl. Dyn. Syst.*, 12, 175–203 (2013).

[Sa02] B. Sandstede. Stability of travelling waves. *Handbook of dynamical systems.* Vol. 2, 983–1055, North-Holland, Amsterdam (2002).

[SS00] B. Sandstede, A. Scheel. Absolute and convective instabilities of waves on unbounded and large bounded domains. *Physica D*, 145, 233-277 (2000).

[SS04] B. Sandstede, A. Scheel. Evans function and blow-up methods in critical eigenvalue problems. *Discr. Cont. Dyn. Sys.*, 10, 941–964 (2004).

[SOBP97] C.P. Schenk, M. Or-Guil, M Bode, H.-G. Purwins. Interacting pulses in three-component reaction-diffusion systems on two-dimensional domains. *Physical Review Letters*, 78, no. 19, 3781–3784 (1997).

[SRW05] W. Sun, M. J. Ward, R. Russell. The slow dynamics of two-spike solutions for the Gray-Scott and Gierer-Meinhardt systems: competition and oscillatory instabilities. *SIAM J. Appl. Dyn. Systems.*, 4, no. 4, 904–953 (2005).

[VE07] V.K. Vanag, I.R. Epstein. Localized patterns in reaction-diffusion systems. *Chaos*, 17, no. 3, 037–110 (2007).

[Zeg07] P.A. Zegeling Theory and Application of Adaptive Moving Grid Methods in "Adaptive Computations: Theory and Algorithms" *S*cience Press, Beijing, 2007, Mathematics Monograph Series 6, p. 279–332 (2007)